Generation of polyclonal antibodies against Theiler's Murine Encephalomyelitis virus protein 2C, and their use in investigating localisation of the protein in infected cells

Dissertation submitted in fulfillment of the requirements for the degree of

Master of Science in Microbiology

At

Rhodes University

By

Tembisa Innocencia Jauka

May 2010

ABSTRACT

The Picornavirus family of positive sense RNA viruses includes some significant human and animal pathogens including Poliovirus (PV), Foot-and-Mouth disease virus (FMDV) and Human Rhinovirus (HRV). The genome is translated within the host cell into a polyprotein that is proteolytically cleaved into the structural and non-structural proteins. The highly conserved, non-structural protein 2C has numerous roles during the virus life cycle and is essential for virus replication. Although the protein has been well studied in the case of PV, its interactions with the host cell during picornavirus infection is poorly understood. Theiler's Encephalomyelitis virus (TMEV) is a picornavirus that infects mice, and is being used in our laboratory as a model in which to study the 2C protein. In this study, polyclonal antibodies against the TMEV 2C protein were generated and used to localise the protein in infected cells by indirect immunofluorescence. To produce antigen for immunisation purposes, the TMEV-2C protein sequence was analysed to identify hydrophilic and antigenic regions. An internal region of the 2C representing amino acid residues 31-210 was selected, expressed in bacteria and purified by nickel NTA affinity chromatography. Time course analysis of 2C (31-210) showed that the peptide was maximally expressed at 5 hours post induction. The peptide was solubilised using a mild detergent and 1.5 mg of purified antigen was used for immunisation of rabbits. Western blot analysis confirmed that the antibodies could detect both bacterially-expressed antigen, and virally-expressed 2C. Examination of virus-infected baby hamster kidney cells by immunofluorescence and confocal microscopy using the anti-serum (anti-TMEV 2C antibodies) showed that the protein had a diffuse distribution upon early infection and at later stages it was located in a large perinuclear structure representing the viral replication complex. Furthermore, 2C localised to the Golgi apparatus as revealed by dual-label immunofluorescence using anti-TMEV 2C antibodies and wheat germ agglutinin (WGA). Furthermore, it was shown that TMEV infection results in changes in cell morphology and a redistribution of the cytoskeletal protein, β-actin. The successful production of antibodies that recognise TMEV 2C opens the way for further studies to investigate interactions between 2C and host-encoded factors.

DECLARATION

I, Tembisa Innocencia Jauka, hereby declare that this thesis is my own unaided work and that, where other people's work has been used it is referenced as such. I further declare that, this work has not been submitted elsewhere for a higher degree application.

Signature: …… Date: ……

Table of contents

Chapter 2: Preparation of antigen for the generation of polyclonal antibodies for detection of TMEV 2C protein

Chapter 3: Detection of 2C in TMEV infected BHK-21 cells

List of Figures

List of Tables

List of abbreviations

AIDS	Acquired immunodeficiency virus
ATPase	Adenosine triphosphatase
BCA	Bicinchoninic Acid
BHK	Baby Hamster Kidney
BSA	Bovine serum albumin
CAR	Coxsackievirus-Adenovirus Receptor
CD55	Decay accelerating protein
CO_2	Carbon dioxide
CPE	Cytopathic effect
DAPI	4, 6-diamidino-2-phenylindole
DMEM	Dulbecco's modified eagles medium
DNA	Deoxyribonucleic acid
EDTA	Ethylenediamineletetraacetate
ELISA	Enzyme-llinked immunosorbent assay
ER	Endoplasmic reticulum
Fab	Fragment antigen binding site
FCS	Fetal calf serum
Fc	Effector region
FDA	Food and Drug Association
GTPase	Guanidine triphosphatase
HIV	Human immunodeficiency virus
h.p.i.	Hours post infection
Igs	Immunoglobulins
IF	Immunofluorescence
IPTG	Isopropyl-β-D-1-thiogalactopyranoside
IRES	Internal ribosome entry site
L	Leader protein
LSCM	Laser Scanning Confocal Microscopy
MAbs	Monoclonal antibodies
MOI	Multiplicity of infection
Min	Minutes
mRNA	Messenger RNA

NTP	Nucleoside triphosphatase
OD_{600nm}	Optical density at 600nm
ORF	Open reading frame
PB	Permeabilisation buffer
PBS	Phosphate-buffered saline
PAbs	Polyclonal antibodies
PEG	Polyethylene glycol
PFU	Plaque forming units
PMSF	Phenylmethyl-sulfonyl fluoride
Poly-A	Poly-adenosine
PSF	Penicillin/streptomycin/fungizone
RER	Rough endoplasmic reticulum
RNA	Ribonucleic acid
RT	Room Temperature
Sarcosyl	N-lauroylsarcosine
SDS-PAGE	Sodium dodecyl sulphate polyacrylamide gel electrophoresis
TAE	Tris acetate
TBS	Tris buffered saline
TBS-T	Tris buffered saline Tween-20
Tntc	Too numerous to count
UTR	Untranslated region
UV	Ultra violet
WB	Western blotting

Viruses

FMDV	Foot-and-Mouth-Disease Virus
HAV	Hepatitis A Virus
HRV	Human Rhino Virus
PV	Poliovirus
TMEV	Theiler's Murine Encephalomyelitis Virus

Units and symbols

α	alpha
β	beta
bp	base pairs
%	percent
°C	degrees Celsius
cm^2	square centimetres
g	gram
kDa	kilo Daltons
l	litre
M	molar
mM	milli molar
mg	milligrams
ml	millilitres
ng	nano grams
nt	nucleotide
rpm	revolutions per minute
µg	micro grams
µl	micro litres
V	Volts

Lists of outputs

Local Conference proceedings:

Jauka, T. and C. Knox. Generation and testing of polyclonal antibodies against TMEV-2C protein. Poster presentation. SASM & BIO2BIZZ 09 conference, held at ICC, Durban September 20-24

Research article:

Tembisa Jauka, Lorraine Mutsvunguma, Aileen Boshoff, Adrienne Edkins and Caroline Knox. Localisation of Theiler's Murine Encephalomyelitis virus protein 2C to the Golgi apparatus during infection using antibodies developed against a peptide region of the protein (in press).

DEDICATION

Dedicated

in loving memory to

My late father, Larry and aunt, Seza

ACKNOWLEDGEMENTS

I would like to extend my sincere thanks to my supervisor**,** Dr Caroline Knox, without whom this project would have not been a success. I am truly grateful to you for all that you have taught me, your patience, understanding nature and always helping me with techniques. I am also thankful for your time and valuable inputs during the writing of my thesis.

To my co-supervisor Dr Aileen Boshoff, I thank you for all your assistance with the preparation of the antigen and proof reading this thesis.

To Dr Adrienne Edkins, thank you for all the time you took off your work to teach me how to use the confocal microscope and help me get good images.

To Mrs Val Hodgson, I am thankful to you for all your advice pertaining to tissue culture.To Dr Petra Gentz, I thank you for your assistance with the antibody testing protocols.

My lab partners Buhle and Lorraine, it was a marvel working with you guys. I will always cherish the good times we had in the lab! Most importantly thank you for taking me in when I needed you most. Annie, thanks for showing me around when I first got to Rhodes and making me feel at home. Rita thanks for being a good friend and always willing to listen.

To Luvuyo, thank you for believing in me, your constant encouragements and understanding. Thank you for being my pillar of strength.

I would like to thank my family for their love, support and encouragement. Mom, without your constant motivation I would have not made it this far. Thanks to my sisters and brothers for believing in me. My baby girl, mommy did this for you!

For Funding, I am grateful to the NRF-research grant and HB-WEBB scholarship.

Above all, I thank God for all His blessings.

1. LITERATURE REVIEW

1.1 Picornaviruses

The word "virus" is derived, from Latin and means poison. Viruses are so small that they cannot be seen under the light microscope and are able to pass through filters used to remove bacteria and other contaminating substances. Viruses are obligate intracellular parasites meaning that they can only reproduce in host cells. More than 4000 different viruses have been identified and they are classified according to structure, nature of their genome, host organisms and disease they cause (Flint *et al.*, 2004; Voyles, 2002).

Picornaviruses are small viruses with a RNA genome and are responsible for a number of significant human and animal diseases. The picornaviruses are currently divided into 12 genera: Aphthovirus, Avihepatovirus, Cardiovirus, Enterovirus, Erbovirus, Hepatovirus, Kobuvirus, Parechovirus, Senecavirus, Sapelovirus, Teschovirus and Tremovirus species (Stanway *et al*., 2005). Diseases caused by some members of these genera are listed in Table 1.1 below. Notable members of the *Picornaviridae* include the Human enterovirus C, of which poliovirus (PV) is one of the serotypes which causes poliomyelitis in humans, Hepatitis A virus (HAV) causes hepatitis, Foot and Mouth disease virus (FMDV) is responsible for infection of cloven hoofed animals and Human Rhinovirus (HRV) which has over 100 serotypes and causes common cold.

Table 1.1; The Picornavirus genera and diseases caused by each species (Bedard and Semler, 2004).

Genus	Species	Disease
Apthovirus	Foot-and Mouth Disease virus	FMD-in cloven hoof animals
Cardiovirus	Theiler's virus	Myelitis in mice
Enterovirus	Poliovirus	Poliomyelitis
Hepatovirus	Hepatitis A virus	Liver disease
Parechovirus	Human parechovirus	Chronic meningoencephalitis
Erbovirus	Equine rhinitis B virus	Upper respiratory diseases
Teschovirus	Porcine teschovirus	Teschen-Talfan-neurological diseases

The diseases caused by the above-mentioned pathogens have diverse economic and health effects. FMDV is notorious for its impacts on economically important livestock. There are seven serotypes of FMDV which have been identified to date, namely; Asia 1, O, A, C, SAT1-3 (Grubman & Baxt, 2004; Oem *et al.*, 2008). In the past, outbreaks caused by FMDV resulted in great economic losses in the agricultural industries as a consequence of animal culling so as to prevent the spread of the disease. One such incident which cost damage of over 8 billion pounds was the outbreak in the United Kingdom in 2001 (Thompson *et al.,* 2002).

Poliovirus, the prototype picornavirus, is responsible for severe poliomyelitis. Although the disease has been eradicated in most countries of the world (Bedard & Semler 2004) some countries such as India, Nigeria, Afghanistan and Pakistan were still reporting cases between the years of 2000 to 2005 (Arita *et al.,* 2006). HRV is an economic pest worldwide which is responsible for upper respiratory tract infections and results in loss of working days. Acquisition of immunity to rhinoviruses is difficult because of the presence of over 100 distinct antigenic serotypes (Fox, 1976; Melnick, 1980). The only form of protection relies on the antibodies produced in the upper respiratory tract (URT) and these do not offer lifelong protection due to the changing genetic make-up of the virus (Fox *et al*., 1985). Hepatitis A virus is transmitted via the fecal-oral route and the liver is the site of infection and results in high cases of morbidity especially in developing countries of the world (Costa-Mattioli *et al.*, 2002). Parechoviruses cause respiratory tract infections, gastroenteritis and central nervous system diseases (Krogerus *et al.,* 2003).

TMEV is a picornavirus belonging to the genus cardiovirus which infects the central nervous system of mice eventually causing demyelination (Lipton, 1975). Virulent strains of TME have been studied intensively as a model for understanding the pathogenesis of multiple sclerosis (Oleszak *et al.*, 2004). TMEV is classified into two groups based on infectivity and the type of disease that it produces following intracerebral inoculation of mice. The two groups are GDVII and Theiler original (TO). The GDVII group is characterised by two strains the GDVII and FA strain and these are more neurovirulent than the TO strain and cause acute fatal encephalitis. The strains, BeAn, DA, WW, TO4 and Yale fall under the TO group and these strains are

less neurovirulent and are responsible for chronic inflammatory demyelinating disease (Lipton & Friedman, 1980).

Due to biosafety reasons TMEV was chosen as a model for this study because it is not pathogenic to humans and thus can be safely used in the laboratory. A study system has been developed whereby TMEV permissively infects and replicates in baby hamster kidney (BHK-21) cells. This cell line is also widely used for diagnostic purposes and vaccine production of FMDV (Barteling, 2004).

1.2 *Picornavirus genome organisation*

Picornaviruses are characterised by a positive sense single-stranded RNA genome packaged into a non-enveloped capsid with icosahedral symmetry. The capsid is made from 60 subunits arranged as 12 pentamers and is approximately 30 nm in diameter. Each subunit consists of four structural proteins namely: VP1, VP2, VP3 and VP4 (Figure 1.1). Three of the structural proteins VP1, VP2 and VP3 are exposed on the surface. VP4 is the smallest capsid protein which is embedded inside the icosahedron structure (Racaniello, 2001).

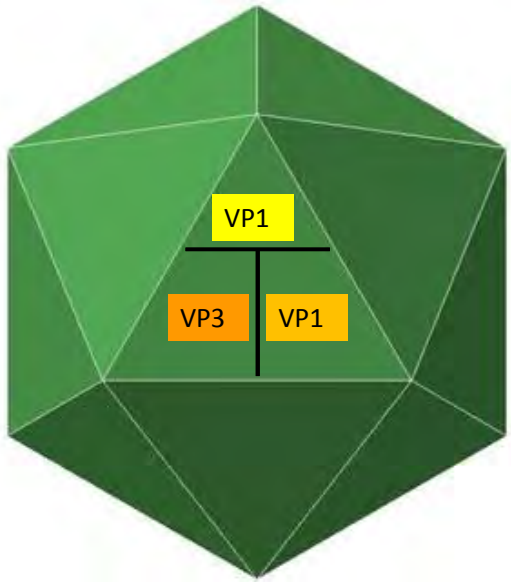

Figure 1.1: Schematic organisation of the picornavirus capsid. The capsid proteins are arranged in an icosahedral symmetry made up of 60 subunits each containing four capsid proteins VP1, VP2, VP3 and VP4. VP1-3 are shown on the surface while VP4 is within the capsid (adapted from Flint *et al.*, 2004).

The picornavirus proteins are encoded in a single, long open reading frame (ORF) of about 7200-8500 kb as shown in Figure 1.2. Picornaviruses are believed to follow a similar replication strategy since they are similar in genome organisation. At the 5′ end of the ORF is a long untranslated region (UTR) of about 600-1200 nucleotides and it is attached to a small protein called VPg which acts as a primer for the viral replicase (Rohll *et al.*, 1995). The 5′ UTR is important for translation, virulence, and encapsidation (Racaniello, 2001). Within the 5′ UTR there is a cloverleaf structure called the Internal Ribosome Entry Site (IRES) (Martínez-Salas *et al.*, 2008). The picornavirus IRES is a sequence that promotes translation initiation of the viral genome while host cell protein translation is shut off and contains extensive regions of RNA secondary structure (Racaniello, 2001). The 3′ UTR is about 50-100 nucleotides long and forms a stem loop structure that is essential for viral replication (Harris *et al*., 1994). The rest of the genome encodes a single polyprotein of between 2100 and 2400 amino acids (Cann, 2005).

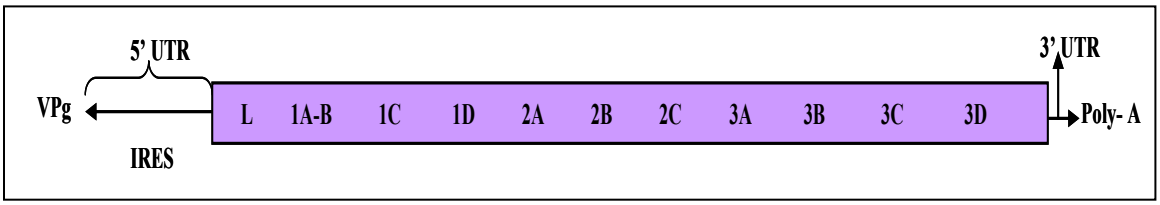

Figure 1.2: Schematic diagram showing genome organisation of picornaviruses. VPg is at the extreme 5′ end of the genome. The IRES element is within the 5′ UTR which is followed by the coding sequences for viral proteins. The 3′ end is polyadenylated (adapted from Martínez-Salas *et al.*, 2008).

1.3 Proteolytic processing of proteins

As mentioned in *section 1.2*, the picornavirus proteins are encoded in a single ORF which is translated within the host cell cytoplasm to form a polyprotein. Several virus-encoded proteases cleave the polyprotein into the structural and non-structural proteins which are encoded by the P1 and P2-P3 domains respectively (Figure 1.3). The 2A protease is responsible for the initial cleavage between the P1 domain and the P2 and P3 domains (Donnelly *et al.*, 1997; Ryan *et al.*, 1991; Sommergruber *et al.*, 1989; Toyoda *et al.*, 1986). Most of the other cleavages are mediated by 3C and 3CD (Bedard & Semler, 2004). The structural proteins 1A, 1B, 1C and 1D are post-translationally cleaved to produce VP1, VP3 and VP0 of the provirion capsid. VP0 is

cleaved to give VP4 and VP2 proteins which form the mature capsid reviewed in (Agol, 2002; Hogle, 2002). 2A, 2B, 2BC, 2C, 3A, 3B, 3CD and 3D are the non-structural proteins and they are responsible for many functions during replication of the viral genome. The non-structural proteins will be discussed in detail in *section 1.5* with a greater emphasis on the 2C protein since it is the focus of this study.

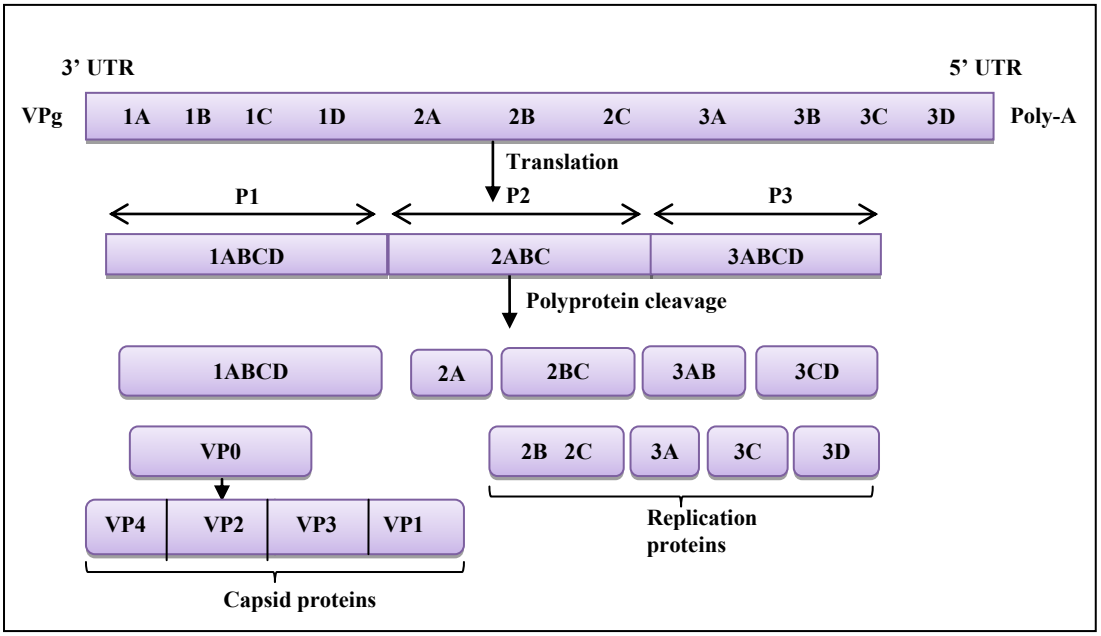

Figure 1.3: Schematic presentation of picornavirus polyprotein processing. The genome encodes its proteins in a single open reading frame and this is translated into a long polyprotein which is consequently cleaved by proteases into three domains P1, P2 and P3 respectively. The P1 domain produces four structural proteins namely; VP1, VP2, VP3 and VP4. The P2 and P3 domains give rise to non-structural proteins 2A, 2B, 2C, 3A , 3B, 3AB, 3C and 3D respectively (adapted from Bedard and Semler, 2004).

1.4 *Picornavirus replication*

The replication of picornavirus occurs in the cytoplasm of infected cells within membrane-bound replication complexes. The infection cycle is initiated by attachment, penetration and uncoating to release the virus particles (Figure 1.4). Picornaviruses use cell surface molecules known as receptors to adhere to membranes of their host cells and different viruses use different receptors while others share the same receptors. For example, PV uses a decay accelerating protein (CD55) as a receptor, coxsackie B virus attaches to the coxsackievirus-adenovirus receptor (Car),

FMDV uses a vitronectin receptor, and HRV uses sialic acid which is a carbohydrate (Flint *et al*., 2004). Following uncoating, the RNA is released into the cytoplasm and begins a round of viral translation. Unlike most host mRNAs, translated viral mRNA does not contain a 7-methyl-Guanidine cap structure at its 5′ end and initiates protein synthesis internally at the IRES (shown in Figure 1.2) by a cap-independent mechanism (Belsham & Brangwyn., 1990; Kuhn *et al.*, 1990). During picornavirus replication, cap-dependent mRNA translation is inhibited as a result of the cleavage of protein synthesis initiation factors (Devaney *et al.*, 1988).

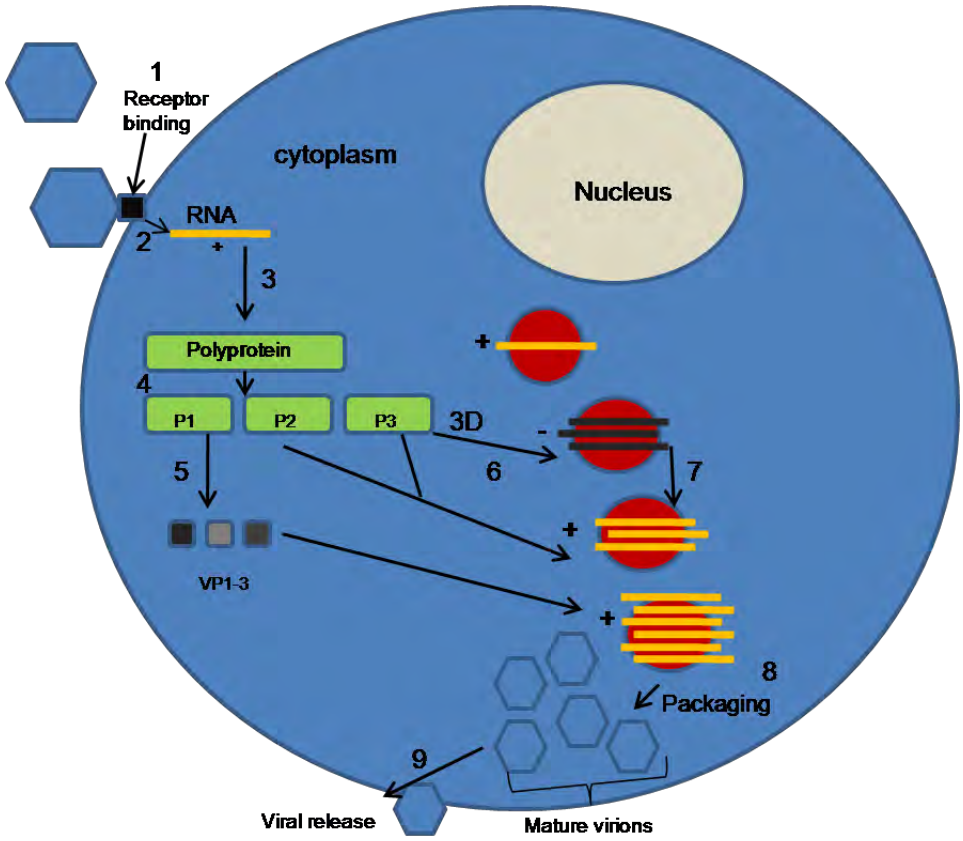

Figure 1.4: **Schematic presentation of picornavirus replication**. Replication occurs in the cytoplasm of infected cells and takes the following order: 1: Attachment of virus particle to host cell receptor followed by penetration into the cell; 2: Uncoating and release of the RNA; 3: Translation of the mRNA to yield the polyprotein, 4: cleavage of the polyprotein into P1, P2 and P3 domains; 5: P1 domain is processed into three capsid proteins (VP1-3); 6: synthesis of the negative sense RNA by 3D polymerase; 7: Synthesis of the positive strand from the negative sense strand; 8: nascent virions are produced and packaged into the capsids and 9 the cell lysis and virions are released (adapted from Flint *et al.*, 2004).

The mRNA is translated to produce first the 3D protein, the RNA-dependent RNA polymerase, which replicates the genome using VPg (3B) as a primer (Crawford & Baltimore, 1983). Subsequently, synthesis of the capsid and non-structural proteins follows. Positive strand RNA acts as a template for the replication of the negative strand which in turn acts as a template for production of nascent positive strand RNA (Flanegan & Baltimore, 1977; Flint *et al.*, 2004). The positive strands are then translated into structural and non-structural proteins on host ribosomes. It is interesting to note that translation and replication are not thought to occur simultaneously during the infectious cycle (Gamarnik & Andino, 1998). Following synthesis of positive RNA strands capsid proteins associate with the RNA and enclose it inside the provirion capsid which is non-infectious. Upon maturation, VP0 is cleaved into VP2 and VP4 to produce infectious virions which are released through cell lysis (Flint *et al.*, 2004).

1.5 The non-structural proteins

Picornavirus non-structural proteins are found within the P2 and P3 domains of the polyprotein and include proteins 2A, 2B, 2BC, 2C, 3A, 3B, 3AB, 3C, 3CD and 3D. These proteins are responsible for targeting and rearranging cellular membranes to create vesicles on which virus replication takes place (Aldabe & Carrasco, 1995; Bienz *et al.*, 1983; Bienz *et al.*, 1990; Cho *et al.*, 1994; Knox *et al.*, 2005; Moffat *et al.*, 2005; Monaghan *et al.*, 2004; Palmenberg *et al.*, 1992; Schlegel *et al.*, 1996; Suhy *et al.*, 2000). The proteins 3A and 3B will be discussed together and the proteins 3C, 3CD and 3D discussed in one section.

1.5.1 2A protein

As mentioned in *section 1.3,* the 2A protein is a protease responsible for the primary cleavage of the P1 domain from the rest of the polyprotein. This strategy differs between picornaviruses (Figure 1.5). For entero and rhinoviruses, this cleavage occurs due to the 2A protein cleaving itself at the N-terminus. In cardioviruses and apthoviruses, 2A protein cleaves the polyprotein between the C terminus of 2A protein and the N terminus of 2B protein, giving rise to a P1-2A precursor protein. The 2A protein of hepato and parechoviruses does not take part in cleaving of the P1

domain, rather $3C^{pro}$ is believed to be responsible for that processing event (Palmenberg *et al.*, 1992; Ryan & Flint, 1997).

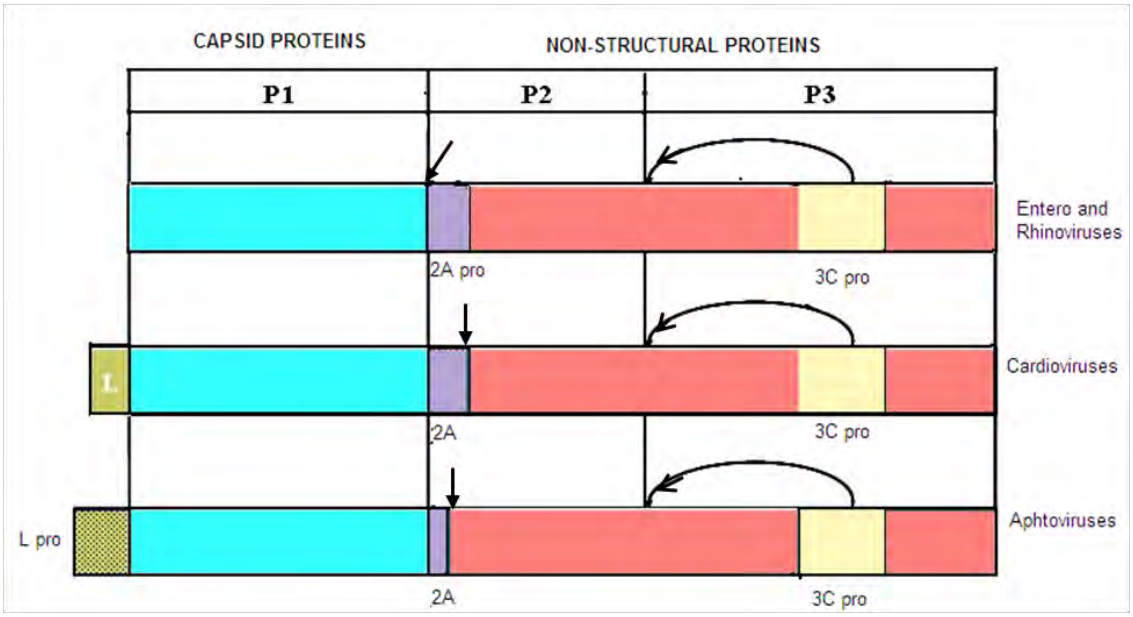

Figure 1.5: Polyprotein processing in picornaviruses. Polyprotein cleavage is carried out by 2A and 3C proteins. In entero-and rhinoviruses the 2A protein cleaves the polyprotein at its N-terminus. In cardio-and apthoviruses the 2A protein cleaves at its C-terminus. The leader (L) of aphtoviruses also has proteolytic activity. The arrows indicate the sites of cleavage by the respective proteins (adapted from Ryan *et al.*, 1991).

1.5.2 2B protein

The picornavirus 2B protein is a small hydrophobic membrane protein of about 100 amino acids situated within the P2 domain. The exact role of 2B during replication is not well defined but mutations within the PV 2B protein resulted in non-complementable defects in viral RNA replication (Johnson & Sarnow, 1991). This may reflect a need for the presence of 2B or 2BC proteins at the site of replication or a disruption of the structure of the viral RNA causing defective RNA synthesis (Bernstein *et al.*, 1986; Johnson & Sarnow, 1991).

Other effects of the picornavirus 2B protein include disassembly of the Golgi complex accompanied by inhibition of protein secretion (Doedens & Kirkegaard, 1995). 2B protein has also been identified as a viroporin, which are hydrophobic proteins

encoded by animal viruses that are able to disturb membrane integrity, resulting in virus egress (Carrasco & Smith, 1976; Nieva *et al.*, 2003) and has been found to alter membrane permeability (Aldabe *et al.*, 1996; de Jong *et al.*, 2006; van Kuppeveld *et al.*, 1997).

1.5.3 2BC protein

The 2BC protein is a membrane-associated precursor of the 2B and 2C proteins. Like 2C protein, 2BC protein has been shown to possess ATPase activity (Wimmer, unpublished data). PV 2BC protein is found within the viral replication complex on the surface of virus-induced vesicles, and when transiently expressed in HeLa and yeast cells, is capable of inducing the proliferation of membranous vesicles (Aldabe & Carrasco, 1995; Barco & Carrasco, 1995; Cho *et al.*, 1994). Moreover, the FMDV 2BC protein modifies the ER and blocks protein transport between the ER and Golgi apparatus (Moffat *et al.*, 2005; Moffat *et al.*, 2007).

1.5.4 The 3A and 3B proteins

These proteins are found in the P3 domain of the genome. 3A protein is a small hydrophobic protein that associates with intracellular membranes (Doedens *et al.*, 1997; Moffat *et al.*, 2005), and it is the cleavage product of the 3AB protein. The 3A protein contains a conserved hydrophobic region of 22 amino acids near its C-terminus, which is responsible for association with membranes (Lee *et al.*, 2006). Transient expression of PV 3A protein has been shown to inhibit ER-to-Golgi protein traffic, resulting in the build up of proteins destined for secretion and the subsequent distortion and swelling of the ER cisternae (Doedens *et al.*, 1997; Suhy *et al.*, 2000). The 3B protein is known as VPg and is covalently linked to the 5′ end of the genome. Three copies of the gene are present in the genomic RNA. 3B protein acts as a primer for RNA synthesis and it is found linked to the 5′ ends of both negative and positive strand RNA (Paul, 2002).

1.5.5 3C, 3CD and 3D proteins

The 3C, 3CD and 3D proteins are found within the P3 domain of picornaviruses. $3C^{pro}$ and 3CD proteins of picornaviruses are multifunctional viral proteases involved in

secondary cleavage events during polyprotein processing (Racaniello, 2001; Skern *et al.*, 2002). They are also involved in binding viral RNA and in replication (Bedard & Semler, 2004). The 3CD protein is a precursor of the viral protease 3C and the viral polymerase 3D. 3C protein functions with 3D protein to stimulate uridylylation of VPg which acts as a primer during replication (Paul *et al.*, 2000). 3CD protein has protease activity but not polymerase activity (Harris *et al.*, 1992). 3D protein is the RNA-dependent RNA polymerase which is responsible for RNA chain elongation during viral RNA synthesis (Flint *et al.*, 2004; Racaniello, 2001).

1.6 2C protein

1.6.1 Conservation of the protein within the picornavirus family

The picornavirus 2C protein is encoded within the P2 domain and is approximately 36 kDa and is the most conserved protein within the *picornaviridae* family (Carrasco *et al.*, 2002; Emini *et al.*, 1985). Amino acid sequence alignments of 2C protein of different picornaviruses show that the protein is highly conserved (Argos *et al.*, 1984). In order to show this conservation, the 2C protein amino acid sequences of different picornaviruses were aligned using the Clustal W Multiple Sequence Alignment Program (Thompson *et al.*, 1994). The program was used on default settings and Gonnet 250 was used to determine the identity matrix. Figure 1.6 shows amino acid sequence alignments of TMEV (Genbank accession number: M20562), FMDV (accession number: NP_740508), PV (accession number: NP_ 740473), HRV (accession number: NP_001552438) and HAV (accession number: NP_740555).

The green coloured residues in Figure 1.6 (shown by the asterisk; *) represent amino acids which are 100% identical and many of these are within the boxed area which represents the NTP binding regions of the protein. This result is in line with previous findings which showed that the 2C protein is highly conserved especially within the NTP domain (Argos *et al.*, 1984; Gorbalenya *et al.*, 1989; Gorbalenya & Koonin, 1989; Gorbalenya *et al.*, 1990). Shown in red (:) are residues which have conserved substitutions. Also observed in the figure are residues which share similar physical and chemical properties and these are shown in yellow (.).

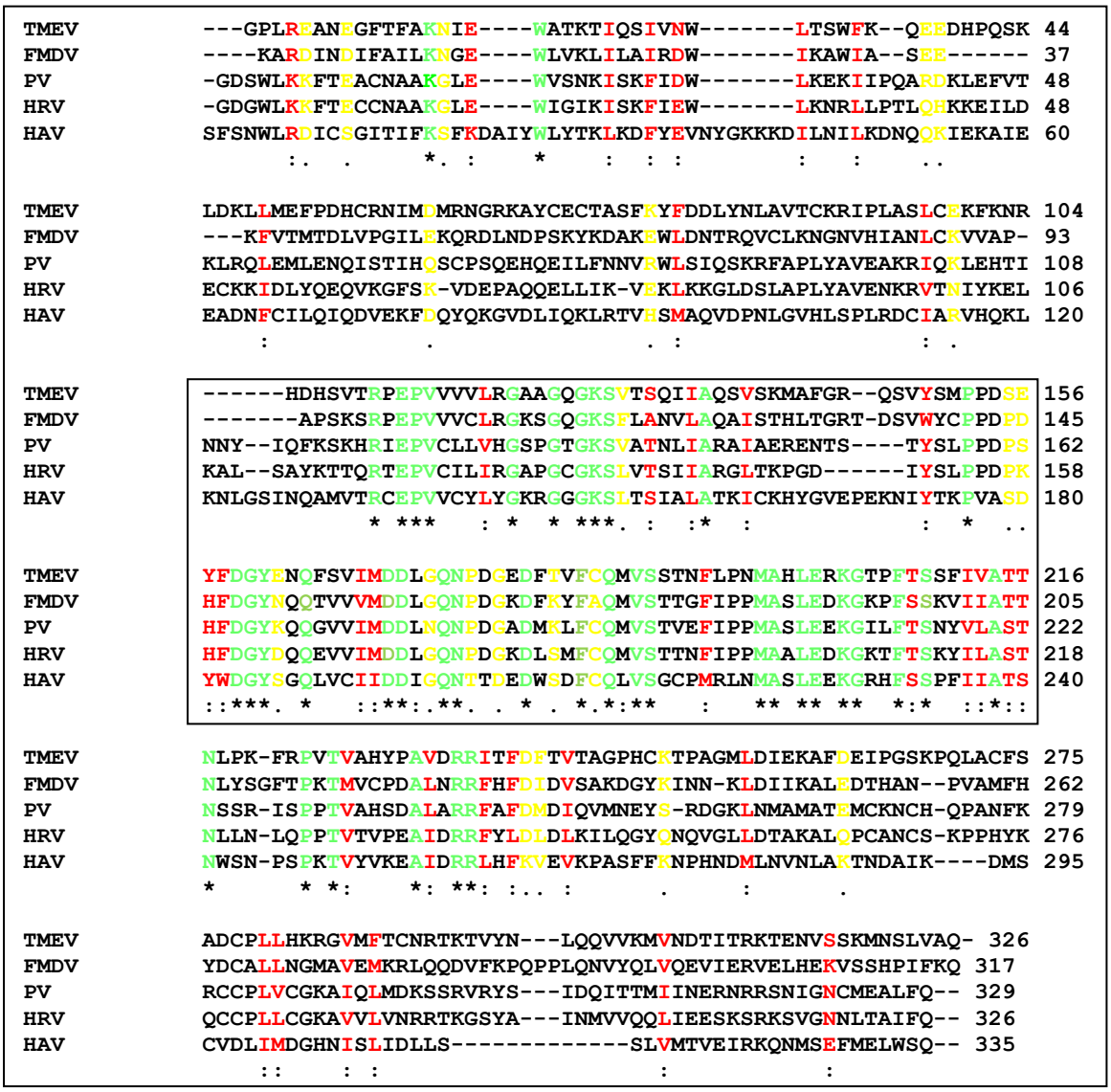

Figure 1.6: Multiple sequence alignment of the picornavirus 2C amino acids were performed using the Clustal W 1.81 program. Residues which are identical in all sequences are indicated by the asteric (***in green**). Most of these conserved residues are concentrated within the NTP binding regions of the proteins (boxed area). Substitution conserved residues are shown by double dots (: in red) and represent up to 75% sequence identity. Single dots (. in yellow) show amino acid residues which have similar physical and chemical properties and have semi conserved substitutions.

1.6.2 Structure and organisation of the 2C protein

The secondary structure of 2C protein is proposed to have three functional domains (Banerjee *et al.*, 2004; Carrasco *et al.*, 2002; Teterina *et al.*, 1997). Figure 1.7 shows a schematic diagram showing the different domains of the PV 2C protein. In orange are the nucleoside triphosphate-binding (NTP) regions. RNA binding and membrane

binding domains are shown in yellow (Rodriguez & Carrasco, 1995). Amphipathic α-helices are present at the N- and C-termini of the protein.

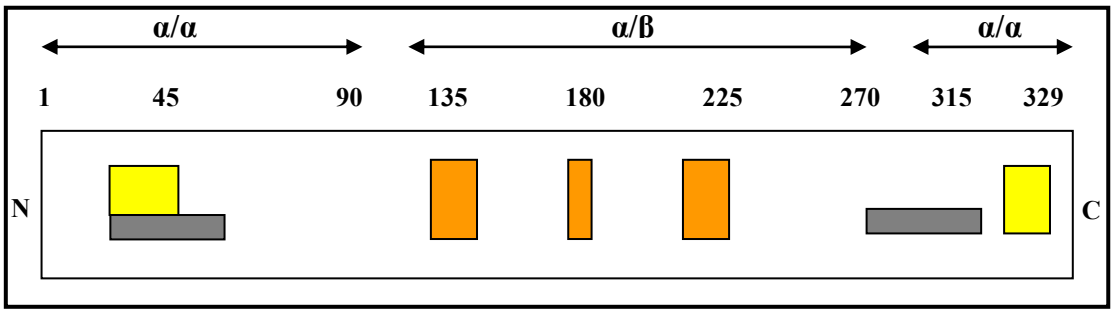

Figure 1.7: Diagrammatic presentation of the structural domains of the PV 2C protein. The diagram shows two RNA binding domains at the N and C-terminus (yellow), membrane binding domain (grey) and the NTP-binding domains (orange). Double-headed arrows show regions of the alpha helices at the N and C-termini and the alpha/beta helix in the central region of the protein (adapted from Banerjee *et al*., 2004).

1.6.3 Functions of the 2C protein

As seen in Figure 1.7, the 2C protein has three different domains of which each gives the protein a specific function. 2C is a multifunctional protein and it has numerous important functions in virus replication. The functions include membrane binding and domains have been identified at both the N- and C-termini of the protein (Echeverri *et al.*, 1998; Echeverri & Dasgupta, 1995; Paul *et al.*, 1994; Teterina *et al.*, 1997; Teterina *et al.*, 2006). Membrane binding activity of the 2C protein has been mapped to the putative class A amphipathic helix at the N-terminus (Paul *et al.*, 1994). By engineering mutations in the N terminal amphiphatic helix, membrane-binding ability was affected (Murray *et al.*, 2009; Paul *et al.*, 1994).

The protein also has RNA binding activity and this occurs due to its amino and carboxyl RNA binding motifs (Banerjee & Dasgupta, 2001; Banerjee *et al.*, 1997; Mirzayan & Wimmer, 1994; Rodriguez & Carrasco, 1995). Using mobility gel shift and UV cross-linking assays it was shown that PV 2C protein interacts with the 3′ cloverleaf structure of the negative strand (Banerjee *et al.*, 2001). The ability of the 2C to bind to membranes and the negative strand RNA suggests that it is involved in anchoring the negative strand RNA to the virus-induced replication complex

(Banerjee & Dasgupta, 2001; Banerjee *et al.*, 2001; Rodriguez & Carrasco, 1993; Rodriguez & Carrasco, 1995).

In addition, the 2C protein also has NTPase activity (Mirzayan & Wimmer, 1994; Rodriguez & Carrasco, 1993; Teterina *et al.*, 1992). Biochemical studies have shown that PV 2C ATPase activity is inhibited by low concentrations of guanidine hydrochloride, an inhibitor of PV RNA replication (Pfister & Wimmer, 1999). The NTP binding domains are necessary for the ATPase activity of the protein in RNA replication (Mirzayan & Wimmer, 1992; Pfister & Wimmer, 1999).

PV 2C protein is implicated in the proliferation of induced membranous vesicles in infected cells that become the site of replication (Aldabe & Carrasco, 1995; Bienz *et al.*, 1987; Bienz *et al.*, 1990., Bienz *et al.*, 1992; Cho *et al.*, 1994; Schlegel *et al.*, 1996). The 2C and 2BC proteins have been shown to induce membrane vesicles similar to those found in infected cells when expressed in the absence of the other viral proteins (Aldabe & Carrasco, 1995; Cho *et al.*, 1994).

Other processes in which 2C protein is implicated includes encapsidation (Vance *et al.*, 1997), regulation of 3C protease activity (Banerjee *et al.*, 2004) and virus uncoating (Li & Baltimore, 1990). Evidence for viral encapsidation by the 2C protein was obtained through use of an antiviral drug, hydantion which inhibits replication in PV cultures. Late in infection the cultures were found to contain new assembly intermediates which resemble those of viral encapsidation intermediates (Vance *et al.,* 1997). PV 2C protein was found to co-immunoprecipitate with viral protease 3C and this resulted in inhibition of the protease activity of the 3C protein both *in vivo* and *in vitro* (Banerjee *et al.*, 2004; Schlegel *et al.*, 1996).

1.7 Origin of membrane vesicles and site of replication

Infection with RNA viruses has been long associated with formation of membrane vesicles which are derived from various cellular components. Membrane vesicles have been found in the cytoplasm of picornavirus-infected cells as a result of intracellular membrane remodelling and these vesicles are required for the replication of viral RNA (Bienz *et al.*, 1992; Guinea & Carrasco, 1990; Rust *et al.*, 2001; Suhy *et*

al., 2000). Insect viruses such as the Flock house virus, induce membranes outside the mitochondria in infected cells (Miller *et al.*, 2001). Brome mosaic virus forms the vesicles found located in the ER of infected barley protoplasts (Restrepo-Hartwig & Ahlquist, 1996). The replication of Semliki Forest and Sindbis virus is located in complex structures associated with modified secondary lysosomes and endosomes (Froshauer *et al.*, 1988). Immunogold labelling, confocal and electron microscopy analysis showed that rubella virus replication complexes are derived from modified lysosomes (Magliano *et al.*, 1998).

Picornaviruses are known to synthesize their genomes in association with newly generated membranous vesicles that proliferate from the mid-phase of infection (Caliguiri & Tamm, 1969; 1970). Electron micrographs of PV-infected cells showed that the membrane vesicles had two lipid membranes and surrounding these vesicles were virus particles (Rust *et al.*, 2001). The membrane vesicles observed in the cytoplasm of PV-infected cells are thought to derive from of the ER (Bienz *et al.*, 1987; Rust *et al.*, 2001). However, Schlegel *et al*., (1996) performed biochemical analyse on cells expressing PV 2C protein and found that these membranes were derived from diverse intracellular organelles, including the endoplasmic reticulum, Golgi apparatus, lysosomes and endosomes. Evidence that these vesicles originate from the membranes of the secretory pathway comes from using brefeldin A, an inhibitor of protein secretion, which was found to inhibit poliovirus RNA synthesis (Irurzun *et al.*, 1992; Maynell *et al.*, 1992). Furthermore, in PV-infected cells, the Golgi apparatus disassembles and the cellular secretory pathway is inhibited (Cho *et al.*, 1994; Doedens & Kirkegaard, 1995; Sandoval & Carrasco, 1997).

1.8 Antibody structure and Function

The focus of this study was to generate polyclonal antibodies against TMEV 2C in order to study the localisation of the protein in infected cells. This section describes briefly what antibodies are and their functions and applications in different settings. Antibodies are serum glycoproteins known as immunoglobulins (Igs) and they are secreted by differentiated B-cells. They are produced in response to molecules and organisms foreign to the host. Antibodies are made of four protein subunits. Two copies of the heavy and light chain are identical and these are held together by

disulfide and noncovalent bonds. The structure of an antibody takes the form of a "Y"–shaped molecule (Figure 1.8). The N-termini of the Y molecule form the antigen binding domains known as Fab regions and these regions vary from one antibody molecule to another, while the C-terminus forms the Fc domain, which defines the class of antibody and determines functional properties. The Fab domain and the Fc regions are connected by a region known as the hinge which imparts lateral and rotational movement of the Fab domain (Janeway *et al.*, 2005; Lipman *et al.*, 2005).

There are five classes of antibodies each having a different function and these are; IgG, IgD, IgE, IgM and IgA. IgG is predominant in serum, it functions to activate the classical complement pathway and binds macrophages and neutrophils for enhancement of phagocytosis. IgD is found on surfaces of B-lymphocytes and mediates B-cell activation and suppression. IgE is found bound to basophils and mast cells where it controls allergic reactions. IgM it is the first to be produced during an immune response and it activates the classical complement pathway. IgA antibodies are mainly secreted by mucosal lymphoid tissues where they protect body surfaces exposed to the environment by blocking entry of bacteria and virus through the mucous membranes (Coico *et al.*, 2003; Janeway *et al.*, 2005).

Antibodies have many functions in humoral immune responses including neutralisation of toxins by blocking the active sites on toxins, agglutination of particulate antigens and precipitation of soluble antigens. Opsonisation is another function of antibodies whereby the antigen is engulfed and destroyed inside the cell by phagocytosis. The complement pathway is activated by binding of antigen or pathogen specific antibodies. Complement activation occurs as a series of steps which leads to the opsonisation and ultimately lysis and/or phagocytosis of the invading organism. Antibody-dependant cell mediated cytotoxicity is another function of antibodies which is activated by binding of the target cell to the Fab region and the Fc region binds to Fc receptors on natural killer cells whereby the natural killer cells are focused on the target cells and are consequently killed (Coico *et al.*, 2003; Janeway *et al.*, 2005; Lipman *et al.*, 2005).

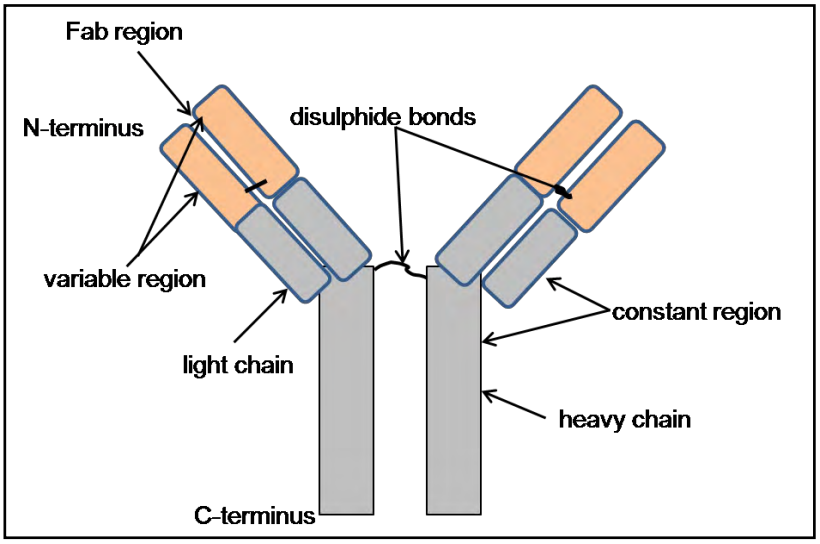

Figure 1.8: Schematic diagram of an antibody molecule. The antibody molecule is composed of two sets of identical heavy and light chains, which make the Y-shaped structure. Each chain contains a constant (grey) and variable (orange) region which are held to together by disulfide bonds. Antigen binding sites are situated in between the amino (N) terminal point and are referred to as fragment antigen binding (Fab). The carboxyl (C) terminus of the two chains fold together to form the effector domains (Fc) (adapted from Janeway *et al.*, 2005).

1.9 Monoclonal versus Polyclonal antibodies

Monoclonal antibodies (MAbs) are derived from a single clone of antibody producing B-cells. They are also produced by injection of mammals with the antigen. The spleen of the animal is then removed and the B cells are fused to immortal myeloma cells forming a hybridoma which is screened by enzyme linked-immunosorbent assay (ELISA). The selected hybridoma is then injected into a second mouse whereby it induces a localised tumor which is full of antibody fluids, which can then be extracted and monoclonal antibodies isolated by column chromatography (Kohler & Milstein, 1975).

Polyclonal antibodies (PAbs) are synthesised by injection of an antigen into a host animal (e.g. goat, rabbit or mouse), harvesting the plasma, and removing clotting factors to produce serum containing the antibodies. As mentioned in *section 1.8,* antibodies are produced in response to antigens by secreting B cells which divide to produce effector cells some of which produce memory cells. Memory B-cells form the basis of immunological memory and ensure a more rapid and effective response

on a second encounter with a pathogen and provides a longer lasting protective immunity. It is for this reason that animals are given booster injections as the first or primary response to antigen does not yield a high titer of the antibody or antibodies with high affinity to the antigen (McCullough & Summerfield, 2005). PAbs are generated much quicker, are less expensive and the skills required to know the technique are less complicated than those for generation of MAbs. PAbs normally have greater specificity than MAbs since they are produced from a large group of B-cell clones (Lipman *et al.*, 2005).

PAbs against the TMEV 2C protein were produced in this study by injection of two rabbits with the 2C antigen. The rabbits were bled three times and the serum was collected and used as antibody.

1.10 Applications of antibodies

Antibodies have been extensively applied for research, therapeutic, and diagnostic purposes for the improvement of the health and welfare of humans and animals. Some applications in research are biochemical and include immunoblotting and immunoprecipitation to detect antigens in samples. ELISA involves the use of enzyme labelled antigens to detect antibodies in samples. Microscopical techniques include Immunofluorescence (IF), immunohistochemistry and electron microscopy (EM) that utilise antibodies to detect antigens in a single cell or in the context of the whole tissue (Bonifacino *et al.*, 2001; Gallagher *et al.*, 1998; Harlow & Lane, 1988; 1999; Hornbeck, 1991).

Antibodies are widely used in virus research and many of the mechanisms by which the virus replicates in host cells could not have been examined without appropriate specific antibodies. For example, as in this particular study, antibodies have been used in IF analysis to localise the site of replication in host cells and also to localise individual viral proteins in order to dissect their functions (Cho *et al.*, 1994; de Jong *et al.*, 2003; de Jong *et al.*, 2008; Doedens & Kirkegaard, 1995; Knox *et al.*, 2005; Moffat *et al.*, 2005; Moffat *et al.*, 2007; Rouiller *et al.*, 1998; Sandoval & Carrasco, 1997; Suhy *et al.*, 2000; van Kuppeveld *et al.*, 1997). Cytoplasmic vesicles have been identified in infected cells using electron microscopy (Bienz *et al.*, 1987; Monaghan

et al., 2004; Schlegel *et al.*, 1996; Suhy *et al.*, 2000). Membrane binding properties of proteins have also been elucidated using antibodies specific to the proteins by immunoprecipitation and immunoblotting (Echeverri *et al.*, 1998; Echeverri & Dasgupta, 1995; Paul *et al.*, 1994; Teterina *et al.*, 2006).

Antibodies are widely used in diagnostic applications. For example, Dot ELISA is an antibody detection assay for immunological diagnosis of patients with neurocysticercosis and is a promising tool for the diagnosis of cysticercosis as a screening test (Agudelo *et al.,* 2005). MAbs also allow rapid detection of hepatitis, influenza, herpes, streptococcal and chlamydia infections (de Soet *et al.*, 1990; Goldstein *et al.*, 1983; Hawkins *et al.*, 1985; Keck *et al.*, 2008; Pothier *et al.*, 1986) . The HIV test is also a diagnostic application where antibodies against the virus are detected using techniques such as immunoprecipitation, Western blot (WB) and ELISA (Cao *et al.*, 1987). PG9 and PG16 antibodies have recently being discovered as neutralizing antibodies for HIV and are being explored for use as effective AIDS vaccine (http://www.physorg.com/news171207257.html).

In therapeutics, MAbs such as Avastin, Humira, Remicade, and Herceptin, among others have been accepted by the FDA and are used to treat different types of cancer ranging from colotectal cancer, breast cancer and kidney cancer (reviewed by Carter, 2001). Mabs have also been used in the treatment of leukaemia, lymphoma and inhibition of angiogenesis (Stephan *et al.*, 2004). Cancer cells were discovered in blood sample using FACs sorting mechanism of CD45 cells using anti-CD45 monoclonal antibodies. This method represents a useful tool in the detection of tumor cells in cancer patients (Baran *et al.,* 1998). MAbs are also used in transplantation to suppress the immune system after organ transplantation (Bumgardner *et al.*, 2001; Koch *et al.*, 2002) and treatment of autoimmune diseases such as diabetes, multiple sclerosis and rheumatoid arthritis which occurs. Some antibodies are widely used in the treatment of graft-versus-host disease and graft rejection in patients receiving bone marrow transplants (Anasetti *et al.*, 1994). Palivizumab (Synagis), an antibody to respiratory synctial virus (RSV), which causes severe illness in newborn infants is used to offer passive immunity (Wu *et al.*, 2008).

1.11 Motivation

The picornavirus 2C protein has been extensively investigated and many studies have shown that it is involved in the proliferation of cytoplasmic membrane vesicles that support virus replication. Many other functions of this protein have been identified, yet the exact molecular mechanism by which it interacts with host cell components is not well understood.

Picornaviruses cause a number of economically important diseases and since their genomes are composed of RNA, they are susceptible to mutation during replication which leads to genetic changes rendering existing vaccines and therapies less effective. An alternative route is developing antiviral agents that specifically target particular interactions between viral and host cell proteins that are essential for replication and assembly. In order to develop such antiviral agents an understanding of these interactions is crucial. Antibodies are essential tools in these types of studies.

1.12 Aims and Objectives

The overall aim of this research was to generate polyclonal antibodies against TMEV 2C protein and use the antibodies to detect and localise the protein in infected cells.

Specific Objectives of the study were to:

- Identify a region of TMEV 2C protein that is potentially hydrophilic and antigenic and thus would elicit an immune response when injected into animals
- To express the peptide in a bacterial system
- To purify the protein by nickel NTA affinity chromatography and provide antigen for immunisation of rabbits
- To test antibodies for their ability to detect bacterially-expressed antigen and 2C protein in infected cell lysates.
- To localise 2C protein in infected cells by indirect immunofluorescence
- To determine changes in the distribution of Golgi markers in infected cells

- To examine the effects of virus infection on cell morphology

2. Preparation of antigen for the generation of polyclonal antibodies for detection of TMEV 2C protein

2.1 Introduction

The lack of an antibody against the TMEV 2C protein has limited our ability to understand the role of the protein during infection and its interaction with the host cell. Although many studies have shown that 2C is essential for virus replication, it is still not clear how it functions during the infectious cycle. Studies which have used epitope tags in order to detect 2C protein have shown that TMEV and FMDV 2C proteins localise to the Golgi apparatus and ER when expressed alone in cells (Bienz *et al.*, 1987; Bienz *et al.*, 1992). Moreover, the FMDV 2C protein targets the Golgi complex in infected cells where it forms part of the replication complex (Knox *et al.*, 2005). No study has described the localisation of TMEV in infected cells because antibodies to detect it are not available. In this chapter, the expression and purification of a peptide region of the TMEV 2C protein for immunisation of rabbits in order to generate polyclonal antibodies is described. The 2C nucleotide sequence was first analysed to predict hydrophobic, hydrophilic and antigenic regions, and amino acids 31-210 were selected for expression and purification. The specific objectives of this chapter were to perform a bioinformatic analysis of the TMEV 2C protein in order to identify hydrophilic and antigenic regions. The next aim was to express the 2C peptide in a bacterial system and purify it for immunisation of rabbits. The final aim was to test the rabbit anti-serum for detection of bacterially-expressed 2C (31-210).

2.2 Materials and Methods

2.2.1 Bacterial strains and growth media

The *E. coli* JM109 bacterial strain was used throughout this study. The cells were stored in 30% glycerol and 0.1 M $CaCl_2$ as stocks at -80°C. Luria Bertani broth (LB; 0.5% NaCl, 0.5% yeast extract, 1% tryptone powder) and Luria Bertani agar (LA) (LB supplemented with 3% bacteriological agar) were used as growth media. Growth of the bacterial strain was carried out at 37°C in LB or LA supplemented with

ampicillin (Amp) at a final concentration of 100 µg/ml. The growth medium will be referred to as LB/Amp and LA/Amp.

2.2.2 Plasmids

Nucleotides 90-630 of the TMEV 2C coding sequence were PCR amplified and cloned into pQE-80L (Qiagen) which had been digested with *Bam* HI and *Hin*d III to create pAST2C4 (created in our laboratory by A. Spracklen). The selected nucleotide region of 2C corresponded to amino acids 31-210 of the protein and the peptide expressed from this plasmid was termed 2C (31-210).

2.2.3 Agarose gel electrophoresis

Agarose gels of 1% (w/v) were prepared in TAE buffer [40 mM Tris (pH 8.0), 0.1% glacial acetic acid, 1 mM EDTA] containing 0.5 µg/ml ethidium bromide. DNA samples were mixed with 6 x loading dye (0.25% bromophenol blue, 40% sucrose) prior to loading. Gels were electrophoresed for 45 minutes (min) at 90 V in TAE buffer. The DNA was visualised by illumination with UV light, and images captured using the Gel Bio-Rad's VersaDoc™ Model 4000 imaging system (Biorad, USA).

2.2.4 Sodium dodecyl-sulphate polyacrylamide gel electrophoresis (SDS-PAGE)

In all experiments, proteins were resolved by 15% SDS-PAGE. Gels were prepared using a 30:1 acrylamide/bisacrylamide reagent (Biorad) according to manufacturer's instructions. Protein samples were prepared for analysis by boiling for 5 min in 5 x SDS-PAGE sample buffer [62.5 mM Tris-HCl (pH 6.8), 10% glycerol, 1.25% bromophenol blue, 0.5% β-mercaptoethanol, 2% SDS]. The gels were electrophoresed at 150 V for 1 hour 45 min in 1 x SDS running buffer [1.44% glycine, 25 mM Tris (pH 8.3), 0.1% SDS]. Gels were stained with Coomassie brilliant blue [6.25% Coomassie (R125), 50% methanol, 10% acetic acid] and then incubated in destain solution (40% methanol, 7% acetic acid).

2.2.5 Western blotting

Proteins separated by SDS-PAGE were transferred onto nitrocellulose Hybond C+ membrane (Amersham Biosciences) in transfer buffer [25 mM Tris-HCl (pH 8), 192 mM glycine, 20% methanol] for 1 hour at 100V on ice with stirring. Prior to the transfer fiber pads and filter paper were pre-soaked in the transfer buffer. In order to determine whether the transfer was successful the membrane was stained with Ponceau-S stain (0.1% Ponceau S in 1% glacial acetic acid) for 2 min. This was followed by rinsing in water and Tris buffered saline [TBS; 150 mM NaCl, 50 mM Tris (pH 7.6)]. The membrane was incubated for 1 hour with shaking or overnight in 5% block [5 g non-fat milk powder in TBS containing 1% Tween (TBS-T)] at 4°C. Primary and secondary antibodies were diluted in 5% block. The membrane was washed with TBS-T in between antibody incubations either 2 x 20 min or 4 x 15 min. Detection was performed using the BM Western blotting chemiluminescence mouse/rabbit kit (Roche) according to manufacturer's instructions. HRP-conjugated secondary antibodies were used at a dilution of 1:12000. Proteins were detected using the VersaDoc™ Model 4000 imaging system (BioRad, USA).

2.2.6 Bioinformatics

In order to successfully prepare an antigen that would elicit an immune response when injected into rabbits and be purified in a bacterial system, a bioinformatic analysis of the 2C protein was performed. The nucleotide sequence of TMEV 2C (strain GDVII) was obtained from the Genbank database (Genbank accession number: M20562). The amino acid sequence of the 2C protein was subjected to the internet-based program Protscale in the Expasytool website (www.expasytool.com) which uses the Kyte and Doolittle method to predict hydrophilic and hydrophobic regions of the protein and the Hopp & Woods method to predict antigenic characters thereof.

2.2.7 Confirmation of integrity of pAST2C4 by restriction analysis and DNA sequencing

pQE-80L was used for the expression and purification of the peptide of interest. The vector consists of an inducible T5 promoter responsible for high expression level of

fusion protein, a polyhistidine tag (His-tag) N-terminal to the multiple cloning site, a replication of origin (ColE1) which allows replication of the plasmid in *E. coli* and the β-lactamase gene which encodes ampicillin resistance. The vector also has a Lac repressor gene (*Lacl*) which ensures that expression of fusion protein does not occur, or is low in the absence of an inducer such as isopropyl-β-D-thiogalactosidase (IPTG).

pAST2C4 (Figure 2.1) was transformed into *E. coli* cells using standard procedures. Plasmid DNA was extracted from overnight cultures inoculated with a single colony using the QIAprep® Spin Miniprep plasmid extraction kit (Qiagen). Integrity of the pAST2C4 construct was confirmed by restriction analysis with *Bam* HI and *Hind* III as these enzymes were used for cloning purposes.

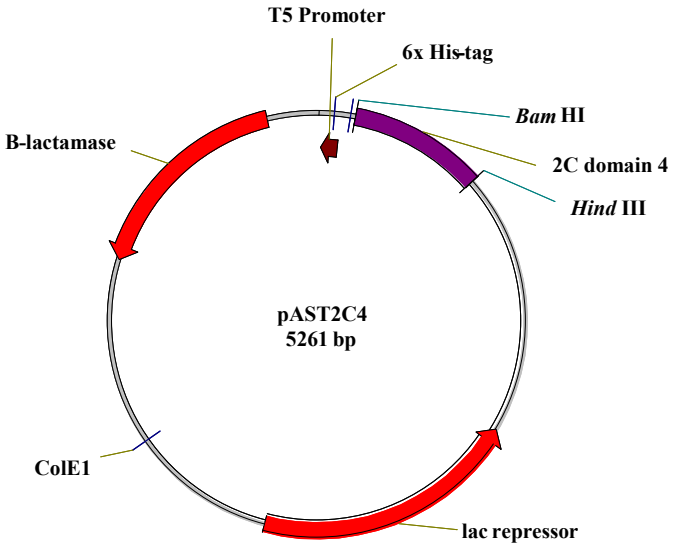

Figure 2.1 Schematic map of pAST2C4. The plasmid was constructed by ligating nucleotides 90-360 of the 2C coding sequence into the multiple cloning site of pQE-80L using *Bam* HI and *Hind* III restriction enzymes.

Digests were analysed by agarose gel electrophoresis in order to estimate fragment sizes. The recombinant plasmid was subjected to DNA sequencing (Inqaba Biotechnology, South Africa) and analysed using Blast to verify that the open reading frame was intact, and that no mutations were generated during the PCR procedure.

2.2.8 Time course of induction

E. coli JM109 cells were transformed with pAST2C4 and pQE-80L using standard procedures. The cells were cultured in LB/Amp at 37°C overnight with aeration. Following overnight incubation, the cultures were diluted 1:10 in LB/Amp and allowed to grow to mid log phase (OD_{600} of 0.6-0.8) at 37°C. The cultures were then induced with IPTG at a final concentration of 1 mM and harvested hourly for 6 hours. 1 ml samples were collected in duplicate, one sample was used for SDS-PAGE analysis to determine protein expression and the other sample to measure cell density. This was done by measuring optical density of the sample at 600 nm using a UV-VIS spectrophotometer (Shimadzu). The cells were harvested by centrifugation at 13000 rpm and the pellet was resuspended in a volume of phosphate buffered saline (PBS) [137 mM NaCl, 2.7 mM KCl, 10 mM Na_2HPO_4, 2 mM KH_2PO_4 (pH 7.4)] as determined by the equation:

Volume of PBS (µl) = A_{600}/0.5 x 150

Samples were prepared for SDS-PAGE and Western analysis using anti-His antibodies (Roche) as described in sections *2.2.4* and *2.2.5* respectively.

2.2.9 Solubility studies

In order to determine whether the truncated 2C peptide (31-210) was soluble, duplicate overnight cultures of *E. coli* cells transformed with pAST2C4 were induced for 5 hours as above. The cultures were harvested by centrifugation at 13000 rpm. One of the pellets was resuspended in 500 µl ice-cold PBS, and the other in PBS containing 7.5% N-lauroylsarcosine (sarcosyl; Sigma) which was prepared as a 20% stock in STE buffer [10 M Tris-HCl (pH 8.0), 150 mM NaCl, 1 mM EDTA]. The cell suspensions were sonicated using Vibra Cell apparatus (Sonics and Materials) at 4°C. Each sample was sonicated for a total of 2 min at 60 A on ice. A 100 µl sample was taken to represent total protein (TP) and the samples clarified by centrifugation to pellet the insoluble fraction. The supernatant or soluble fraction (SF) was collected and the pellet (P) was resuspended in 500 µl PBS. The samples collected were boiled in SDS-sample buffer and stored at -20°C for later analysis by SDS-PAGE.

2.2.10 Purification of 2C (31-210) by Ni-NTA affinity chromatography

Having established the optimum time for protein expression in section *2.2.8*, the culture volume was scaled up to 1 L in order to obtain sufficient peptide antigen for immunisation of rabbits. 250 ml aliquots were harvested in a JA-14 centrifuge rotor at 14000 rpm for 10 min. The pellets were resuspended in 5 ml lysis buffer [50 mM NaH_2PO_4, 300 mM NaCl, 10 mM imidazole (pH 8.0)] and stored at -20°C overnight. Prior to sonication, lysozyme, PMSF and sarcosyl were added to a final concentration of 1 mg/ml, 1 mM and 7.5% respectively. After 30 min incubation at room temperature (RT), samples were sonicated as described above. A sample representing total protein was taken as before, boiled in SDS sample buffer and stored at -20°C. The samples were then clarified by centrifugation at 14000 rpm for 1 min to obtain the soluble fraction. Pellets (insoluble fraction) were discarded.

The supernatants were pooled and mixed with 50% slurry of nickel-charged beads (in a ratio of 200 µl beads/ml of supernatant) which was prepared by charging Sepharose beads (Amersham Biosciences) with 0.1 M $NiSO_4$. Briefly, beads were resuspended in lysis buffer and sedimented by centrifugation at 4000 rpm for 2 min. The supernatant was removed, and a 0.5 bead volume of 0.1 M $NiSO_4$ was added, followed by incubation for 30 min at RT. The beads were sedimented by centrifugation and the supernatant removed. The beads were washed three times with double-distilled H_2O, and centrifuged to sediment the charged beads. The beads were then resuspended in one volume of lysis buffer and stored at 4°C until use. Samples were incubated with the beads for 3 hours with shaking followed by an overnight incubation at 4°C and then washed three times in 10 ml wash buffer [50 mM NaH_2PO_4, 300 mM NaCl, 20 mM imidazole (pH 8.0)], followed by centrifugation at 4000 rpm for 2 min. Wash fractions (W1, W2 and W3) were collected. The protein was eluted in 2 ml elution buffer [50 mM NaH_2PO_4, 300 mM NaCl, 250 mM imidazole, (pH 8.0)] for 1 min on ice with shaking and then centrifuged at 14000 rpm for 2 min. The elution step was repeated three times and samples were collected after each step (E1, E2 and E3). Samples collected during the purification procedure were analysed by SDS-PAGE and stained as described in section *2.2.4*. Protein concentration was determined using the Bicinchoninic Acid (BCA) Kit for protein concentration (Sigma) according to the manufacturer's protocol. In total, 1.5 mg of

purified 2C (31-210) peptide was used for immunization of rabbits by Professor D. U. Bellstedt, Department of Biochemistry, University of Stellenbosch, South Africa.

2.2.11 Testing of Day 0 and Day 44 serum

Approximately 6 weeks after immunisation, antiserum collected at day 0 (pre-immune), 29 and 44 post immunisation was received. The antiserum was tested for its ability to recognise bacterial expressed 2C (31-210) peptide. Firstly, day 0 serum was tested in order to determine whether the rabbit serum contained antibodies which could cross-react with 2C (31-210) peptide. Bacterial cultures harbouring pAST2C4 and pQE-80L were induced for 5 hours with IPTG as described in section *2.2.8*. Crude cell lysates were prepared by boiling in SDS sample buffer and samples were resolved in duplicate by SDS-PAGE. Proteins were transferred to nitrocellulose and one membrane was probed with Day 0 serum at dilution of 1:1000. The other membrane was cut into four strips and probed with Day 44 serum at dilutions of 1:1000, 1:10000, 1:100000 and 1:1000000 in order to determine the optimal antibody concentration for subsequent experiments. To determine sensitivity of the Day 44 serum, different amounts of purified 2C (31-210) peptide ranging between 29 and 232 ng were resolved by SDS-PAGE. Proteins were detected by staining using Coomassie brilliant blue or transferred onto nitrocellulose membrane for Western blot analysis using Day 44 antiserum at a dilution of 1:10000.

2.3 Results and Discussion

2.3.1 Prediction of hydrophilic, hydrophobic and antigenic regions of 2C protein

The TMEV 2C protein sequence was analysed using the internet based program Protscale to predict hydrophobic, hydrophilic and antigenic regions of the protein**.** The aim of these analyses was to predict a region of the protein which is hydrophilic and more likely to be exposed on the surface of the protein in its tertiary conformation. The protein appears to have numerous hydrophobic and hydrophilic regions with no defined domains of either hydrophobicity or hydrophilicity (Figure 2.2). This is surprising as the amino-terminal region of the 2C protein forms an

amphipathic α-helix (Paul *et al.*, 1994) and is involved in membrane binding (Echeverri *et al.*, 1998; Echeverri & Dasgupta, 1995) and the C-terminus of the protein is thought to be involved in membrane binding (Echeverri *et al.*, 1998; Teterina *et al.*, 1997).

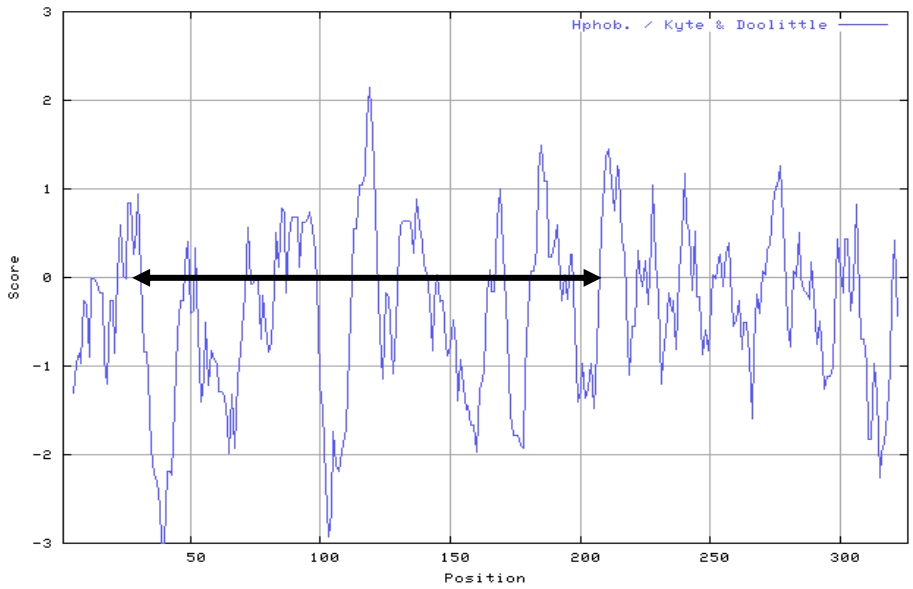

Figure 2.2: Kyte & Doolittle hydrophobic and hydrophilic plot of TMEV 2C. Peaks which are below zero are predicted to be hydrophilic and those above zero are predicted to be hydrophobic regions. Highlighted by the arrow is the region of 2C that was selected for antigen preparation.

Figure 2.2 shows the full-length 2C protein and highlighted by the arrow is an internal region of the protein which predominantly contains hydrophilic regions as seen by peaks below the zero axis. It is necessary that the antigen used for antibody production is capable of eliciting an immune response in the host. An antigenic plot of the 2C protein was generated using Protscale to predict such antigenic regions. Figure 2.3 is a Hopp & Woods plot showing the antigenic characters of 2C. The N-terminus of the protein contains few predicted antigenic characters. The region highlighted by the arrow is potentially antigenic as indicated by peaks above the zero line, and peaks tend to correspond to regions of predicted hydrophilicity shown in Figure 2.2. On the basis of these results, amino acid residues 31-210 were selected for expression and purification in order to produce antigen. The peptide is referred to as 2C (31-210).

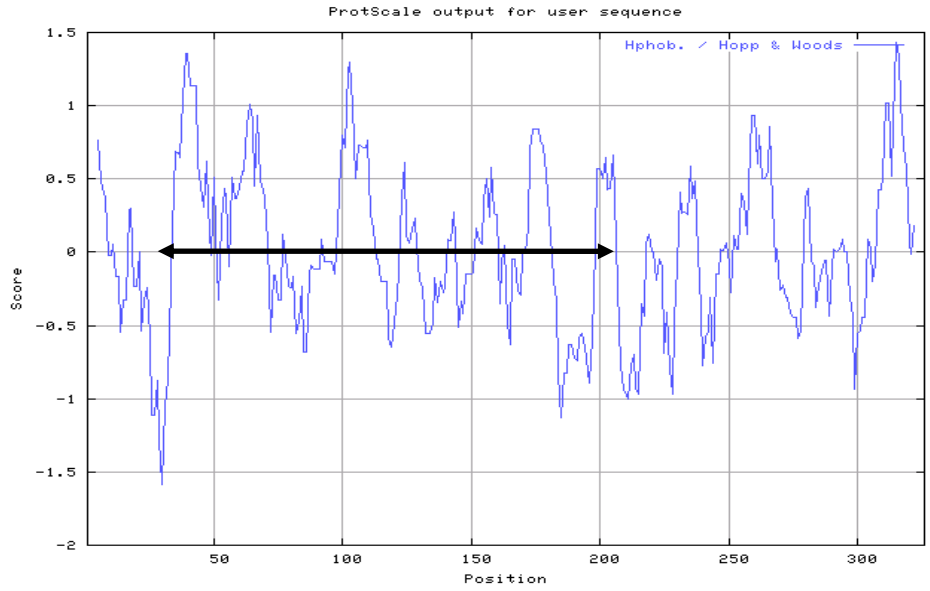

Figure 2.3: Hopp & Woods antigenic plot of TMEV 2C. The regions of the protein below the zero value are predicted to be hydrophobic and non-antigenic. Regions above zero contain predicted antigenic characters. Highlighted by the arrow is the region of the protein that was selected for antigen preparation.

2.3.2 Confirmation of pAST2C4 by restriction analysis

To determine the integrity of pAST2C4, the plasmid and vector were digested with *Bam* HI and *Hind* III and analysed by agarose gel electrophoresis. The results are shown in Figure 2.4. The size of the pAST2C4 is 5261 nucleotides and that of pQE-80L is 4751 nucleotides.

Figure 2.4 shows that when the vector is digested with the two enzymes the result is a linear fragment corresponding to the size of pQE-80L (lane 4). For pAST2C4, we expected the double digest to result in two DNA fragments, one running above the 4000 bp marker and the other just above 500 bp (lane 5). The larger fragment corresponds to the 4751 bp of linearised pQE-80L, and the smaller one to a 540 bp fragment representing nucleotides 90-630 of 2C. Lane 1 contains the kb DNA ladder, and Lanes 2 and 3 undigested pQE80L and pAST2C4 respectively.

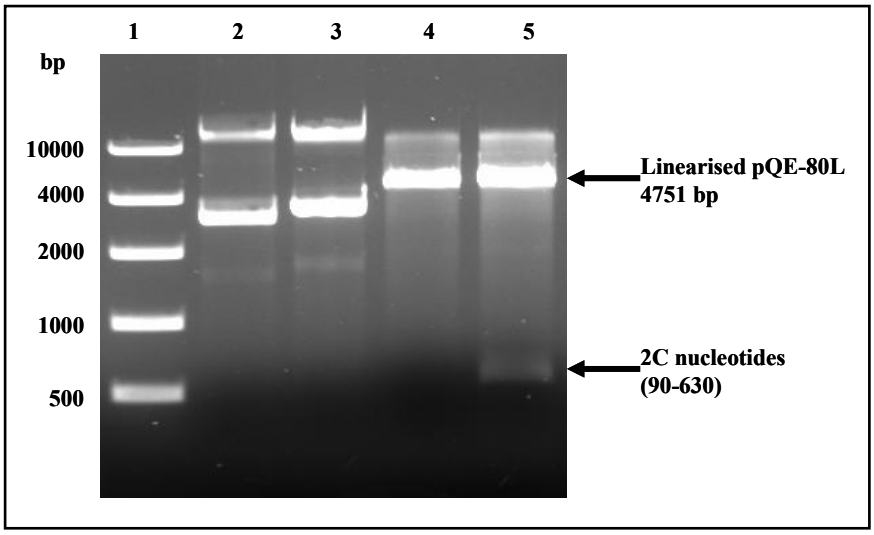

Figure 2.4: Restriction analysis of pQE80L and pAST2C4 confirming the presence of 2C (90-630) in pAST2C4. Lane 1: DNA ladder in base pairs (bp) (Fermentas); lane 2: undigested pQE-80L; lane 3: undigested pAST2C4; lane 4: pQE-80L digested with *Bam* HI and *Hind* III; lane 5: pAST2C4 digested with *Bam* HI and *Hind* III showing the linearized vector and a band just above the 500 bp marker representing nucleotides 90-630 of the 2C sequence (540 bp).

To further examine the integrity of pAST2C4, DNA sequencing was carried out and the results are shown in Figure 2.5 below. The analysis showed that the open reading frame was correct when nucleotides were read in triplicate from the start codon (green) through the histidine tag (blue) to the stop codon, tga (red). Furthermore, the sequence contained no mutations when compared with the TMEV 2C sequence (Genbank accession number: M20562) using BLAST.

atgagaggatcgcatcaccatcaccatcacggatccactagctggttcaagcaggaagaggacc
acccccaatcaaaattagacaaattgcttatggaattccccgatcattgtaggaacattatggatatga
ggaacggtcgaaaggcctattgtgaatgcactgcttcctttaagtattttgatgatctttacaatcttgct
gttacttgcaaaagaattccattagcctccctttgtgagaaatttaagaatagacacgaccactctgtca
ccagacccgagccggtggttgtcatcctgcgcggcgccgctgggcaaggcaaatctgtgaccagc
caaatcattgcccaatctgtttctaagatggcctttggccgtcagtctgtttattctatgcccccgattc
ggaatattttgatggctatgaaaatcaattttctgtgattatggatgatctaggacaaatcccgatggtga
agatttcaccgtcttttgtcaatggtttctagcacaaattttctcccgaatatggctcacctggaaagaaa
aggcacccctttcacctctagctgaaagcttaattag

Figure 2.5: Integrity of pAST2C4 as confirmed by DNA sequencing. Shown in green is the start codon, in blue is the 6x histidine tag upstream of the sequence for 2C (31-210). The *Bam* HI restriction site and *Hind* III restriction sites are shown in brown and yellow respectively. Underlined in black are the forward and reverse primers. The stop codon is shown in red.

2.3.3 Time course of induction

To analyse the expression of 2C (31-210) over time, *E. coli* cultures harbouring pAST2C4 and pQE80L were grown to mid-log phase and induced with 1 mM IPTG for six hours. Samples collected were analysed by SDS-PAGE with Coomassie staining **(**Figure 2.6, panel A).

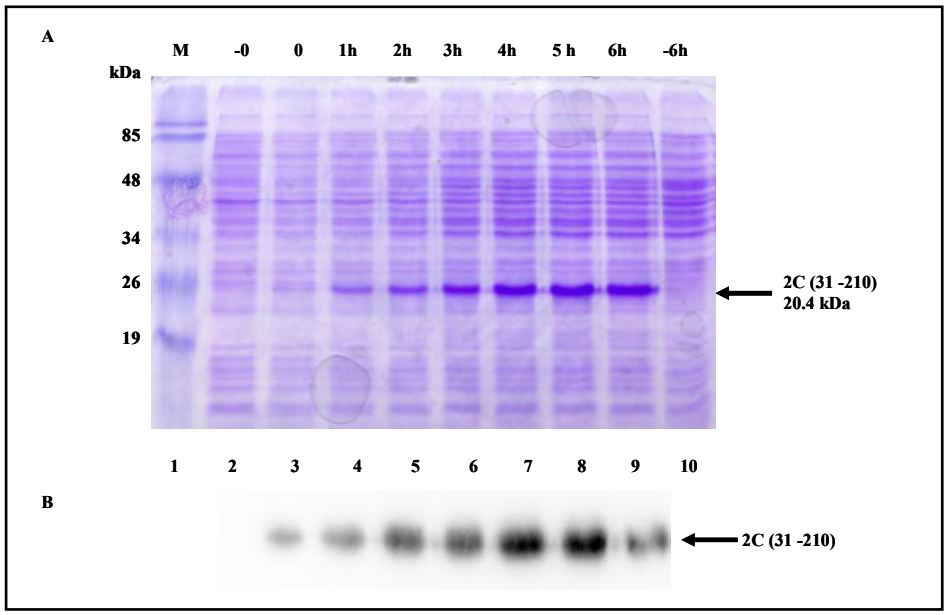

Figure 2.6: Time course of 2C (31-210) expression. Cells were induced and cultivated for 6 hours, samples collected hourly and subjected to 15% SDS-PAGE (A) and Western blotting (B) using anti-His antibodies. Lane 1: protein molecular weight marker in kDa. Lane 2: uninduced cells harbouring pQE-80L (-0); lane 3: cells expressing 2C (31-210) prior to induction; lanes 4-9: cells expressing 2C (31-210) 1 h-6 h post-induction; lane 1 0: cells harbouring pQE-80L at 6 h post-induction.

2C (31-210) expression was detectable at 1 hour post-induction and levels increased with time reaching a maximum at around 5 hours (lanes 3-9). The peptide is not evident in lane 3 before induction as expected. Moreover, the peptide was not present in lanes 2 and 10, which contain lysate from cells harbouring pQE-80L before induction (-0) and at 6 hours (-6) post-induction respectively. To confirm that the peptide present in lanes 3-9 was indeed 2C (31-210), Western blotting was performed using anti-His antibodies (Figure 2.6, panel B). The Western blot result shows that 2C (31-210) can be detected between 0 and 6 hours post-induction, with the maximal expression at 5 hours.

2.3.4 Solubility analysis

The results of the time course experiment showed that 2C (31-210) was maximally expressed at 5 hours post-induction. Therefore, cultures were cultured for 5 hours after induction in order to perform a solubility analysis of the peptide. Cells expressing 2C (31-210) were collected and resuspended in lysis buffer with (Figure 2.7 B) and without 7.5% sarcosyl (Figure 2.7 A) prior to sonication. A sample was taken to represent total protein (TP) before clarifying the sonicates by centrifugation to obtain soluble (S) and pellet (P) fractions. TP, S and P samples were analysed by SDS-PAGE and the results are presented in Figure 2.7.

Figure 2.7 (A) clearly shows that 2C (31-210) is present in the insoluble fraction (compare lanes 2 and 3). This result was undesirable although not unexpected since the Kyte and Doolittle plot previously showed that the protein has both hydrophilic and hydrophobic regions within the sequence chosen. It could also be that the protein is located within inclusion bodies in the cytoplasm because of the high level of expression.

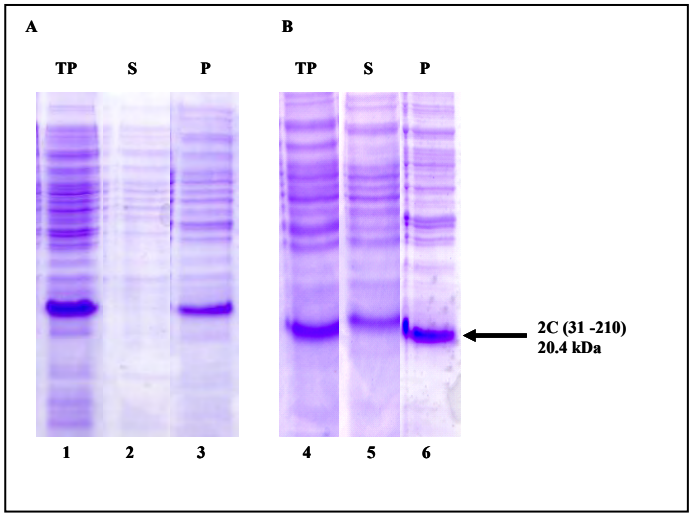

Figure 2.7: Solubility analysis of 2C (31-210). Cells expressing 2C (31-210) were collected and sonicated at 5 hours post-induction in the absence (A) or presence (B) of 7.5% sarcosyl. Samples were clarified to obtain soluble (S) and pellet (P) fractions and resolved by 15% SDS-PAGE. Lane 1: total protein 5 hours post-induction after sonication; lane 2: soluble fraction; lane 3: pellet fraction. Lanes 4-6 contain fractions sonicated after the addition of 7.5% sarcosyl. Lane 4: total protein; lane 5: soluble fraction; lane 6: pellet fraction.

In an attempt to solubilise 2C (31-210), cultures were treated with 7.5% sarcosyl prior to sonication. Sarcosyl is a mild anionic detergent which disrupts cell membranes and thus releases membrane bound proteins. Following treatment with 7.5% sarcosyl, some of the peptide appeared in the soluble fraction (compare lanes 5 and 6). Although a significant amount of the peptide remained in the pellet fraction (lane 6), it was decided to upscale protein expression to produce sufficient amounts of peptide for immunisation.

2.3.5 Large scale protein production and purification

With the aim of producing 1 mg of antigen for immunization of rabbits, the culture was scaled up to 1 L. Following induction for 5 hours, the cells were pelleted, resuspended in lysis buffer supplemented with 7.5% sarcosyl and sonicated at 4°C. Sonicated samples were pooled and clarified by centrifugation at 14000 rpm. Supernatants were mixed with nickel-charged beads in order to purify the peptide. Samples collected during purification steps were analysed by SDS-PAGE (Figure 2.8).

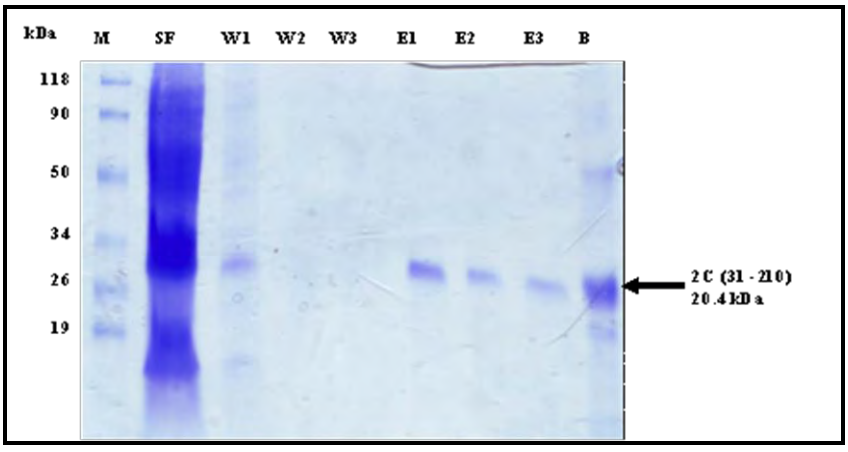

Figure 2.8: SDS-PAGE analysis of purification of 2C (31-210) by nickel affinity chromatography. Samples collected at various stages during the purification procedure were resolved by 15% SDS-PAGE. In lane 1: protein molecular weight marker; lane 2: total soluble protein following sonication and centrifugation (SF); lanes 3-5: wash fractions (W1-W3); lanes 6-8: elution fractions (E1-E3); lane 9: bead fraction (B).

Lane 2 contains total protein after sonication (SF). Numerous proteins are present as expected, with the dominant protein being 2C (31-210) running about the 20.4 kDa

band. The beads were washed 3 times in wash buffer containing 20 mM imidazole. The low concentration of imidazole in wash buffer ensured that proteins that were not bound to the beads or those that were weakly bound by their histidine residues to the beads could be easily washed away. This concentration was low enough to not remove histidine-tagged 2C (31-210). Three elution steps were performed in elution buffer containing 250 mM imidazole. The increase in imidazole concentration results in disruption of the histidine-nickel interaction which results dissociation of the protein. The wash fractions (lanes 3-5) indicate that some 2C (31-210) was lost in the first wash (lane 3) but not in subsequent washes. The peptide was eluted three times with a buffer containing 250 mM imidazole (lanes 6-8). The eluted fractions contained 2C (31-210) with most of the peptide being eluted in the first step (lane 6). The eluted fractions contained 2C (31-210) without any visible contaminating proteins. The bead sample (lane 10) indicates that a substantial amount of the peptide is still bound to the beads following elution. In an attempt to remove more of the peptide from the beads, the concentration of imidazole was increased to 500 mM in the elution buffer and the eluent dialysed against a large volume of PBS, followed by concentration using polyethylene glycol (PEG). This proved unsuccessful as the peptide precipitated during the concentration procedure forming a white precipitate. Since 250 mM imidazole is tolerated by the rabbits (personal communication, Professor D. U Bellstedt), no further attempt was made to dialyse the eluted peptide. The peptide was quantified using the BCA method, and 1.5 mg of purified 2C (31-210) was sent to the University of Stellenbosch for immunisation of rabbits.

2.3.6 Testing of Day 0 and Day 44 serum

a) Specificity testing

To test for cross-reacting antibodies in the pre-immune serum, Western blotting was performed using Day 0 serum at a dilution of 1:1000. As expected, no 2C (31-210) or cellular proteins were detected (data not shown). Day 44 serum was tested by Western blotting at different dilutions using crude cell lysate for its ability to detect 2C (31-210) and to confirm that antibodies against 2C (31-210) were predominant in the serum.

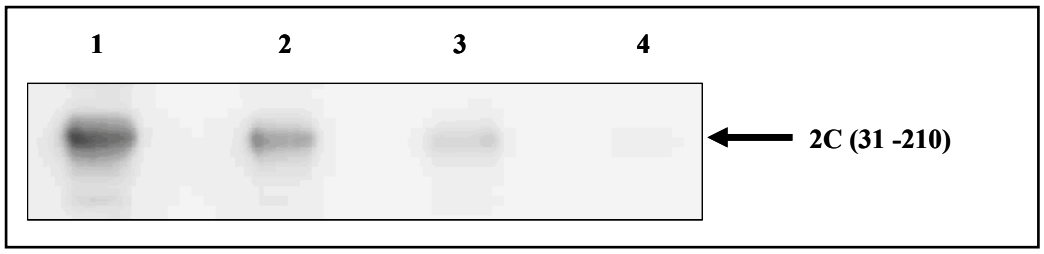

Figure 2.9: Detection of 2C (31-210) using Day 44 serum at different dilutions. Equal amounts of 2C (31-210) were resolved by 15% SDS-PAGE and the peptides transferred to nitrocellulose membrane. Following transfer the membrane was cut into 4 strips and subjected to Western blotting using Day 44 serum at dilutions of 1:1000 (lane 1), 1:10000 (lane 2), 1:100000 (lane 3) and 1:1000000 (lane 4).

Figure 2.9 shows that 2C (31-210) was detected at all dilutions and that signal intensity decreased with increasing dilution of the serum (Lanes 1-4). No other protein bands were observed on the blot. These results confirmed that the serum contained anti 2C (31-210) antibodies. The Day 44 serum will be referred to as anti-TMEV 2C antibodies from here onwards.

b) Sensitivity testing

From the above results, it was decided to apply the anti-TMEV 2C antibodies at a dilution of 1:10000 for subsequent tests. Sensitivity testing was done by resolving various amounts of purified 2C (31-210) by SDS-PAGE (A) and performing Western blotting (B) using anti-TMEV 2C antibodies (Figure 2.10).

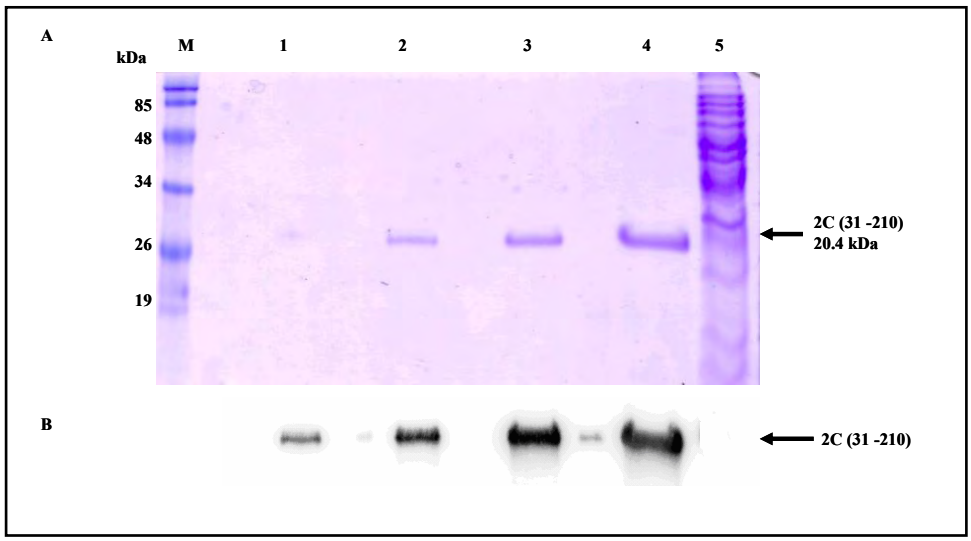

Figure 2.10: Sensitivity testing of anti-TMEV 2C antibodies at 1:10000 dilution. Different concentrations of 2C (31-210) were resolved by 15% SDS-PAGE and stained with Coomassie brilliant blue (A). The bottom image is Western blotting (B) analysis of purified 2C (31-210) using anti-TMEV 2C antibodies. Lanes 1-4: 29, 58, 116 and 232 ng of purified 2C (31-210). Lane 5: lysate harbouring pQE-80L.

Panel A shows increasing amounts of 2C (31-210) visible by Coomassie staining (lanes 1-4). As seen in panel B, anti-TMEV 2C antibodies were highly sensitive in that they could detect as little as 29 ng of purified peptide following a 30 second exposure (lane 1). As the amount of peptide loaded onto the gel was increased, the signal became stronger (lanes 2-5). As expected 2C (31-210) was not detected in lysate harbouring pQE-80L (lane 5).

2.4 Conclusions

The preparation of antigen for immunisation of rabbits in order to generate polyclonal antibodies against TMEV 2C is described in this chapter. A bioinformatic analysis of TMEV 2C was carried out and showed that hydrophilic and hydrophobic regions were present in the sequence. The N- and C-terminal regions of the protein were found to be hydrophobic consistent with studies showing that these domains of the protein are responsible for membrane binding. An internal region of 2C (residues 31-210) was predominantly hydrophilic and antigenic as determined by the Kyte-Doolittle and Hopp-Woods plots, and this was selected for antigen preparation. 2C (31-210) was

successfully expressed from pAST2C4 in a bacterial system. The peptide was maximally expressed 5 hours post induction and detected using anti-His antibodies by Western blotting. Solubility studies showed that the peptide was present in the pellet fraction and not in the supernatant fraction. However, some of the peptide was solubilised following treatment with 7.5% sarcosyl. Nickel affinity purification of the peptide was successful as the peptide was obtained in pure form with no contaminating proteins. Following elution, most of the peptide was still bound to the beads, however the amount purified was sufficient for immunisation of rabbits. Rabbit antiserum was obtained and could detect bacterially-expressed antigen and no cross reacting antibodies were present in the serum. The anti-TMEV 2C antibodies were able to detect the antigen at dilution as a high as 1:1000000, but a 1:10000 dilution was determined to be optimal for detection of purified 2C (31-210). Sensitivity tests showed the antibody to be highly sensitive by detecting as little as 29 ng of purified 2C (31-210). Having established that the anti-TMEV 2C antibodies detect bacterial antigen, we sought to test the antibody for its ability to detect virally-expressed protein as described in the next chapter.

3. Detection of 2C in TMEV infected BHK-21 cells

3.1 Introduction

In this chapter the detection of virally expressed 2C protein in infected BHK-21 cells is described. These cells were chosen as the cell line for experiments as they support TMEV replication. Although studies have been performed on TMEV 2C when expressed alone in cells, it is important to study the protein with other viral proteins involved so as to help elucidate the function of the protein during infection. The use of anti-TMEV 2C antibodies to detect viral protein by Western blotting of infected cell lysates is described. The antibodies were optimized for indirect immunofluorescence analysis in order to localise the protein in infected cells by laser scanning confocal microscopy (LSCM). 2C protein is essential for virus replication and in the case of PV it is found in association with viral replication complexes on the surface of induced vesicles (Domingo & Holland, 1997). When expressed alone in cells, both TMEV and FMDV 2C proteins localise to Golgi membranes (Moffat *et al.*, 2005; Murray *et al.*, 2009). The anti-TMEV 2C antibodies we generated were able to detect 2C in infected cell lysates by Western blotting and in infected cells by indirect immunofluorescence. The distribution of 2C was found to differ during infection. Early on, 2C is distributed in the perinuclear region and as infection progresses it is concentrated on one side of the nucleus suggesting a Golgi localisation.

3.2 Material and methods

3.2.1 Cell Culture

BHK-21 cells were a kind gift of Professor Martin Ryan (University of St Andrews, UK). The cells were maintained in complete medium Dulbecco's modified Eagle's medium (DMEM, Lonza Ltd) supplemented with 5% fetal bovine serum (FBS, Sigma) and 1% penicillin, streptomycin and fungizone (PSF, Invitrogen) in 25 cm^2 vented flasks at 37°C with 10% CO_2.

3.2.2 Subculture of cells

Cells at 100% confluency were rinsed with warm trypsin (Sigma). 1 ml trypsin was added to the monolayer followed by swirling for 1 min, and then excess trypsin was poured off. The flask was incubated at 37°C for a few min to allow cells to detach from the surface. 2 ml of complete medium was added to the flask and the cells were dispersed by pipetting. Cells were subcultured in 25 cm^2 tissue culture flasks containing 7 ml of complete medium.

3.2.3 Cryopreservation of BHK-21 cells

For preservation of cells, a confluent 25 cm^2 flask was subcultured into ten 25 cm^2 flasks as described above. When the cells were 100% confluent, they were trypsinised and resuspended in 1 ml complete medium per flask. The cells were collected in sterile Eppendorf tubes by centrifugation at 1000 rpm for 1 min. The medium was aspirated and the pellet resuspended in 1 ml cryopreservation solution (20% FBS, 10% glycerol, 1% PSF). The cells were stored in 1 ml aliquots in cryovials at -80°C.

3.2.4 Preparation of TMEV stock

A 100% confluent monolayer on a 25 cm^2 flask was subcultured into a 75 cm^2 flask with 15 ml complete medium. When 100% confluency was reached the cells were infected with 1 ml TMEV stock (previously prepared by L. Murray, Rhodes University). The medium was poured off and the cells rinsed with serum-free DMEM. The virus stock was mixed with 4 ml of serum-free DMEM, poured onto the cells and virus adsorption was allowed to occur by shaking at 37°C for 1 hour. The medium in the flask was made up to 10 ml with serum-free DMEM and the flask was incubated overnight at 37°C with 10% CO_2. The cells were lysed by three cycles of freeze-thawing and then collected in a 15 ml falcon tube. Cell debris was pelleted at 1000 rpm for a min and 1 ml virus aliquots stored in cryovials at -80°C.

3.2.5 Titration of TMEV stock by plaque assay

BHK-21 cells were grown to 90-100% confluency in 6 well plates in complete medium at 37°C with 10% CO_2. The virus was prepared as a series of ten-fold dilutions in serum-free DMEM. The medium was aspirated and 1 ml of virus stock

dilutions between 10^{-3} and 10^{-8} was added to each well. Virus adsorption occurred at 37°C with shaking for 1 hour. Virus stocks were aspirated and cells washed with serum-free DMEM and 3 ml overlay solution [50% DMEM, 1.25% methocel (Fluka), 60 mM NaCl in sterile water] was added to each well. The cells were incubated at 37°C with 10% CO_2 for 48 hours until zones of clearance (plaques) were visible when viewed under the light microscope. When the plaques had formed the overlay solution was removed by washing cells gently with PBS (pH 7.4). Cells were fixed with 4% paraformaldehyde at RT for 20 min and washed once with PBS. The plaques were visualised by staining with Coomassie staining solution (45% methanol, 10% glacial acetic acid, 0.002% Coomassie Brilliant Blue) for 20 min at RT. Cells were rinsed with water and the plaques were seen as clear zones on the cell monolayer. The clear zones were counted and the virus titre determined as plaque forming units per millilitre (pfu/ml) taking the dilution factor into account.

3.2.6 Preparation of BHK-21 cell lysate for Western blot analysis

A 100% confluent 25 cm^2 tissue culture flask of BHK-21 cells was subcultured into two 75 cm^2 flasks in complete medium and incubated at 37°C with 10% CO_2 until the cells were 100% confluent. The medium was poured off and the cells washed with serum-free DMEM. One flask was infected with TMEV at a multiplicity of infection (MOI) of 15 and virus adsorption was carried out at 37°C with shaking for 1 hour in 5 ml serum-free DMEM. The other flask was mock-infected with 5 ml serum-free DMEM containing no virus. The flasks were incubated for 5 hours to allow for virus replication and protein expression. The cells were trypsinised at 5 hour post infection (hpi) and collected by centrifugation at 4000 rpm for 1 min. The cells were washed with PBS and resuspended in 200 µl lysis buffer [150 mM tris (pH 7.4), 100 mM NaCl, 0.5% DOC, 1 mM EDTA, 1 mM PMSF, 1% Triton X100, 1 mM Na_2VO_3]. The cells were incubated on ice for 30 min with vortexing every 5 min and then passed through a 25-gauge needle 20 times. The cells were clarified to collect supernatant (soluble fraction) by centrifugation at 13000 rpm for 1 min and the pellet (insoluble fraction) resuspended in 200 µl lysis buffer. Proteins were denatured by boiling in SDS-sample buffer, resolved by 15% SDS-PAGE and transferred onto nitrocellulose membrane for Western blot analysis using anti-TMEV 2C antibodies at 1:200 dilution.

3.2.7 Preparation of cells BHK-21 cells for Immunofluorescence

Cells were grown on sterile 13 mm glass coverslips (VWR International) in a 6-well plate containing complete medium and incubated overnight at 37°C with 10% CO_2. The medium was aspirated and the cells washed twice with serum-free DMEM. Cells were infected with TMEV stock diluted 1:2 in serum-free DMEM (final volume, 1 ml) at a MOI of 100. Control cells were mock-infected with serum-free DMEM. The cells were incubated at 37°C for 30 min with shaking. Virus inoculum was aspirated and the cells were washed with serum-free DMEM. 3 ml of serum-free DMEM was aliquoted into each well and the plates were incubated at 37°C for 8 hours to allow virus replication. The medium was removed and the cells washed with PBS. Coverslips were dipped in ice-cold methanol to fix the cells, air-dried and transferred into the wells of a 24-well plate for immunofluorescence staining.

3.2.8 Indirect immunofluorescence staining of infected cells

Cells were permeabilised in PB (10% sucrose, 1% Triton X100 in PBS) for 20 min with shaking at RT. The cells were blocked in PB containing 2% BSA for 30 min shaking at RT. To optimize the antibody for immunofluorescence analysis, the cells were incubated with anti-TMEV 2C antibodies at dilutions of 1:500, 1:1000 and 1:5000 made up in blocking buffer, and incubated for 1 hour at 37°C with shakig. Cells were washed with wash buffer (PBS containing 0.1% Tween-20) three times for 5 min with shaking. Alexa-Fluor 488-conjugated anti-rabbit secondary antibodies (Invitrogen) were used to detect primary antibodies at a dilution of 1:500. Cells were incubated for 30 min with secondary antibodies in blocking buffer with shaking at RT. This was followed by three 10 min wash steps. To stain the nucleus, 4', 6-Diamino-2-phenylindole dihydrochloride (DAPI, Sigma) was added at a final concentration of 0.8 µg/ml in the second wash. The coverslips were mounted using Vectashield Hard Set Fluorescent Mounting Medium (Vector Laboratories) and stored at 4°C before examination by confocal microscopy.

3.2.9 Confocal microscopy and image acquisition

Cells were visualised using an inverted LSM 510-Meta confocal laser scanning microscope (Zeiss) using the 63x oil immersion objective lens. The helium/neon and argon lasers at wavelengths of 488 and 405 nm were used to excite Alexa fluor 488

and DAPI respectively. All images were analysed using Axiovision LE or SE freeware software (Zeiss) and processed using Photostudio 5 software (Cannon). Images in this thesis have been saved onto a disc (at the back of the thesis) for visualisation purposes.

3.3 Results and discussion

3.3.1 Titration of TMEV stock by plaque assay

The plaque assay is used to quantify infectious virus particles so that MOI can be determined. MOI refers to the number of infectious virus particles per cell. When a monolayer of cells is infected with 1 ml of virus and there are 1000 infectious particles and 1000 cells in that monolayer, then MOI is 1. TME virus was titred to determine pfu/ml in order to calculate MOI for infection experiments. This was done by infecting a 100% confluent monolayer of BHK-21 cells in a 6 well plate with TMEV at dilution between 10^{-3} and 10^{-8}. The results obtained following plaque assay performed on TMEV infected cells are shown in Table 3.1.

Table 3.1: Titration of TMEV virus stock by plaque assay. A 100% monolayer of BHK-21 cells was infected with TMEV at dilutions of 10^{-3}, 10^{-4}, 10^{-5}, 10^{-6}, 10^{-7} and 10^{-8} respectively. Following 30 min incubation with the virus the medium was removed and methocel added to the wells. Subsequently after 48 hour of incubation at 37°C, the cells were stained with Coomassie and plaques were counted and expressed as pfu/ml.

Dilution	No. of Plaques	Pfu/ml (*)
10^{-3}	Clear	0
10^{-4}	Clear	0
10^{-5}	tntc(**)	tntc
10^{-6}	78	78×10^{6}
10^{-7}	26	26×10^{7}
10^{-8}	19	19×10^{8}

(*) Pfu/ml: plaque forming units per millilitre, (**) tntc: too numerous to count

The replication of picornaviruses like other RNA viruses is error prone due to the lack of proof-reading ability of the RNA-dependent RNA polymerase, 3D. Error frequencies have been determined to be as high as 1 in 10^{3} to 10^{4} nucleotides. Due to

these errors, mutations accumulate during replication of the genome and results in the existence of the virus population as a quasi-species. Thus, during infection, only a small percentage of the particles in a virus stock are viable. For PV, it has been shown that not more than 1% of the virions can undergo the infectious cycle (Voyles, 2002). The results shown in Table 3.1 show that there was clearing of the monolayer with dilutions of 10^{-3} to 10^{-4} and that at a dilution of 10^{-5} the monolayer had numerous plaques which were not countable. These results mean that there were more virus particles relative to the number of cells and therefore, even after immobilisation of the virus with methocel, the monolayer cleared. Each cell in the monolayer is infected by one infectious particle and following replication and lysis that particular cell lyses. The new virions released then infect neighbouring cells and results in formation of plaques that can be counted. Because the virus medium was replaced with a solid methocel medium the new virus particles produced cannot move very far from the site in which they were produced. 78 plaques were counted for the 10^{-6} dilution, 26 were visible with the dilution of 10^{-7} and 19 at the 10^{-8} dilution. The values were averaged and the titre of the virus stock was calculated as 7×10^8 pfu/ml.

3.3.2 Detection of 2C protein in infected BHK-21 cell lysates by Western blotting

To test the ability of anti-TMEV 2C antibodies to detect 2C protein in infected BHK-21 cells, a lysate was prepared. Cells grown in a 75 cm^2 flask were infected with TMEV at a MOI of 100, and a second flask mock-infected. The cells were incubated for 5 hours at 37°C with 10% CO_2 and collected by trypsinisation. Supernatant and pellet fractions were separated by centrifugation at 13000 rpm for 1 min and the pellet was resuspended in lysis buffer. The supernatant and pellet fractions were analysed by SDS-PAGE and Western blotting using anti-TMEV 2C antibodies at a dilution of 1:200 (Figure 3.1).

Lanes 2 and 3 of Figure 3.1 contain bacterially-expressed 2C (31-210) and 2C (31-326) respectively. 2C (31-326) was expressed from pBM2C and was created by B. Moyo by cloning nucleotides 90-978 of the 2C coding sequence into pQE-80L, and is an N-terminal truncation of the full length 2C protein. It was used to investigate whether anti-TMEV 2C antibodies could detect the full-length protein. The molecular weight of 2C (31-326) was approximately 34 kDa and the full-length protein

predicted to be 37 kDa. In lane 3, a strong signal was observed for a protein running below the 26 kDa mark and represents residual 2C (31-210) which was not totally removed when the beads were reused. It is not advisable to reuse the nickel beads due to contamination with other proteins.

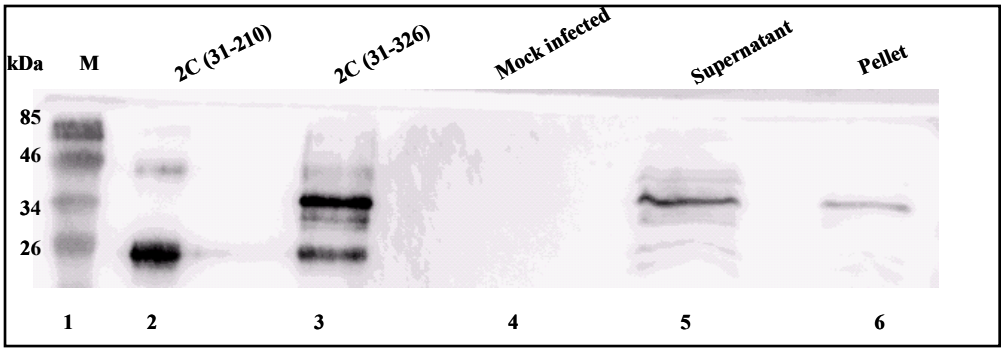

Figure 3.1: Western blot analysis of infected and mock infected cell lysate using anti-TMEV 2C antibodies. Lane 1: protein marker; lane 2: 2C (31-210); lane 3:2C (31-326); lane 4: mock-infected BHK-21 cell lysate; lane 5: supernatant fraction of infected lysate; lane 6: pellet fraction of infected lysate. Anti-TMEV 2C antibodies were used at a 1:200 dilution.

Lane 4 contains mock-infected lysate, and lanes 5 and 6, are the supernatant and pellet fractions from infected lysate respectively. At dilutions of 1:500, 1:1000 and 1:10000, no proteins were detected using anti-TMEV 2C antibodies (data not shown). When applied at a dilution of 1:200, the anti-TMEV 2C antibodies were effective in detecting virally-expressed protein as indicated in Figure 3.1 (lanes 5 and 6). The protein was found both in the supernatant and pellet fractions, running at a position between the 34 and 46 kDa size markers, indicating that it is both soluble and membrane-bound. Interestingly, this result is consistent with that observed for FMDV 2C protein in infected cells in which 2C protein was also found present in soluble and membrane fractions (Knox *et al.*, 2005). As expected, the protein was not detected in mock-infected cell lysates (lane 4) confirming that the protein was present as a result of virus infection. As seen in lanes 2 and 3, the antibodies detected both 2C (31-210) which was used as antigen, and also 2C (31-326). Since the antigen was prepared using a shorter region of the 2C protein it was very interesting to observe that the antibodies were also effective in recognising (almost) full length 2C (31-326). This result was vital in the next experiments where the antibodies will be applied in indirect immunofluorescence to detect full-length, virally-expressed protein.

3.3.3 Detection of 2C in infected cells by indirect immunofluorescence and confocal microscopy

To optimise the anti-TMEV 2C antibodies for application in immunofluorescence analysis of TMEV infected cells, BHK-21 cells were grown on glass coverslips and infected with TMEV at MOI of 100. Cells were fixed with methanol and stained with anti-TMEV 2C antibodies at dilutions ranging between 1:500 and 1:5000. The primary antibodies were detected with Alexa-Fluor 488-conjugated anti-rabbit secondary antibodies. Figure 3.2 shows images obtained by confocal microscopy.

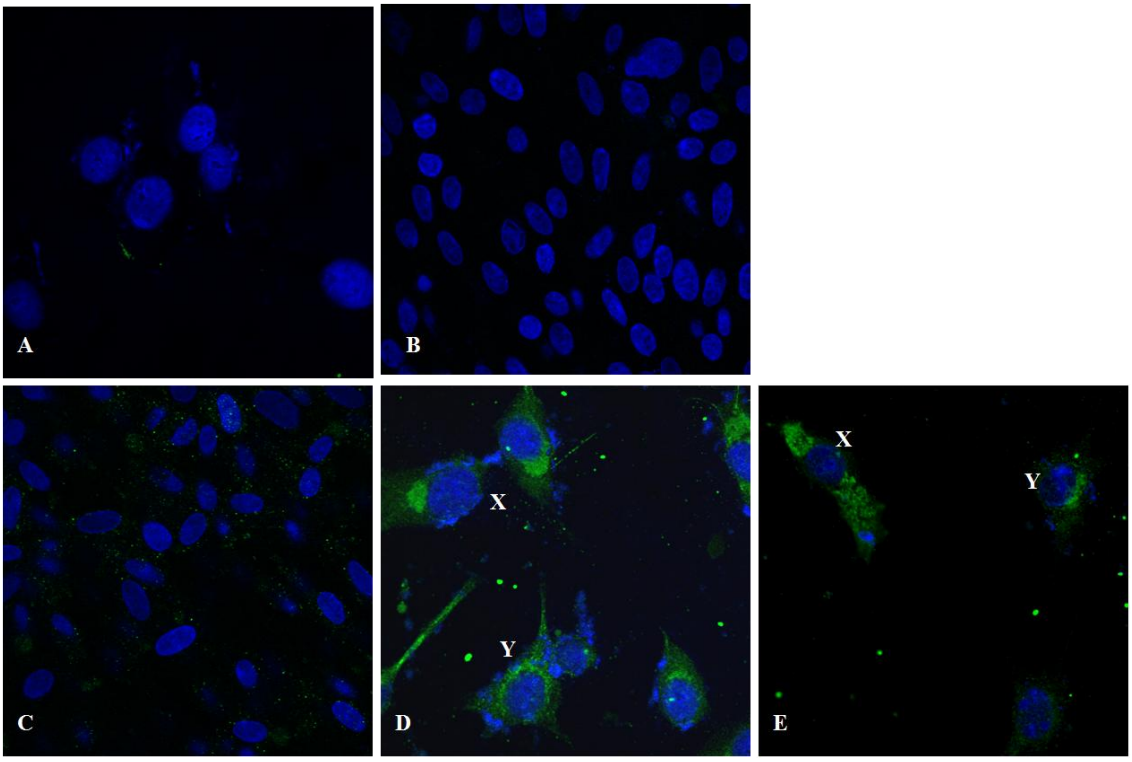

Figure 3.2: Detection of TMEV 2C in infected BHK-21 cells at 8 hpi. A: Uninfected cells were labelled with anti-TMEV 2C antibodies at 1:1000 dilution. **B:** infected cells probed with secondary antibodies only. TMEV 2C was detected with anti-TMEV 2C antibodies at dilutions of 1:5000 (**C**) 1:1000 (**D**) and 1:500 (**E**). Primary antibodies were visualised with Alexa-Fluor 488-conjugate anti-rabbit antibodies. X and Y represent cells at different stages of infection.

At 8 hpi the majority of cells were in advanced stages of CPE and rounded up. However, a few cells were observed which still showed typical fibroblast morphology. Figure 3.2 shows cells with both types of morphology. No signal was detected in uninfected cells at a dilution of 1:1000 (panel A) or when cells were incubated with secondary antibodies alone (panel B). A weak signal was observed

when antibodies were applied at 1:5000 dilution (panel C). At lower dilutions of 1:500 and 1:1000 (panels D and E respectively) a positive signal for 2C protein was observed. The fact that no signal was observed in panels A and B confirms that this signal is as a result of virus infection and also that anti-TMEV 2C antibodies were binding specifically to the 2C protein.

2C protein was located in perinuclear structures in all cells examined. Some cells also showed diffuse cytoplasmic staining which may represent an earlier stage of infection. Since there was some background staining at a dilution of 1:500 (panel D), anti-2C antibodies were used at a dilution of 1:1000 for all subsequent experiments. In panels D and E, there appear to be two different distributions of 2C protein. In the cells labelled X, the 2C protein is situated next to the nucleus in a compact structure while in the cells labelled Y, 2C protein has a diffuse cytoplasmic staining. These distributions could represent different stages of infection with Y being an earlier time point compared to X. This was also observed for FMDV in infected cells where 2C protein showed a cytoplasmic distribution early in infection and later on was found in the perinuclear region (Knox *et al.*, 2005).

3.4 Conclusions

In this chapter, anti-TMEV 2C antibodies were used to detect 2C protein in infected cells by Western blotting and indirect immunofluorescence. A plaque assay was performed to determine the number of infectious virus particles in the stock that was prepared in order to infect the cells at a high MOI. The results showed that virus stocks contained about 10^8 plaque forming units per millilitre of stock. The antibodies could detect 2C protein in cell lysate at 5 hpi at a dilution of 1:200 by Western blotting. Interestingly, fractionation experiments showed that the protein is present in both the soluble and insoluble fractions. This result is consistent with the bioinformatics analysis carried out in chapter 2 which revealed that the protein contains hydrophobic domains which may be associated with membranes. Anti-TMEV 2C antibodies were then optimised for use in immunofluorescence staining and confocal microscopy to detect 2C protein in infected cells. At a dilution of 1:5000, a weak signal for 2C protein was observed. At a 1:500 dilution there was a strong signal with some background staining. It was decided therefore to use a 1:1000

dilution for all subsequent experiments. Two different distributions of 2C protein were observed in infected cells. In some cells, the signal was perinuclear with diffuse cytoplasmic staining, and this may represent an early stage of infection. In other cells, the protein was concentrated on one side of the nucleus with no apparent cytoplasmic staining. This distribution is most probably associated with the later stages of infection. Because the staining pattern resembled that of the Golgi apparatus, experiments were performed in an attempt to investigate this possibility, and are the subject of the following chapter.

4. Localisation of TMEV 2C protein in infected cells

4.1 Introduction

Substantial information has been generated regarding localisation of the 2C protein and its effect during infection through studies conducted on PV and FMDV (Aldabe & Carrasco, 1995; Bienz *et al.*, 1987; Bienz *et al.*, 1990; Bienz *et al.*, 1992; Cho *et al.*, 1994; Knox *et al.*, 2005; Moffat *et al.*, 2007; Schlegel *et al.*, 1996). However, the localisation of TMEV 2C protein in infected cells has not been studied to date and only one study has described the effects of infection on cell morphology (Nédellec *et al.*, 1998). Having established that TMEV 2C protein is localised to the perinuclear region of infected cells as described in chapter 3, the next experiments were conducted to determine if the protein was targeting the Golgi apparatus. The main aim of the experiments described in this chapter was therefore to determine the localisation of 2C protein in infected cells with respect to this organelle by indirect immunofluorescence and confocal microscopy using the anti-TMEV 2C antibodies. At the time of this study; the anti-β-COP antibodies were the only Golgi antibodies available in the laboratory. These could not be used in dual label immunofluorescence experiments with the anti-TMEV 2C antibodies as they were both raised in rabbits. Wheat Germ Agglutinin (WGA), a lectin conjugated to Alexa-Fluor 555 has been widely used to stain Golgi apparatus and membranes of the secretory pathway (Allen *et al.,* 1989, Wright, 1984) was tested in this chapter for it's ability to stain the Golgi apparatus of BHK-21 cells. The first aim was to establish whether WGA could be used as a Golgi marker, and the second to determine the localisation of 2C protein with respect to WGA. A further objective of this chapter was to investigate changes in morphology of TMEV-infected cells by staining cells with antibodies against β-actin at different stages of infection.

4.2 Materials and Methods

4.2.1 Antibodies and Stains

Anti-TMEV 2C antibodies were used at a dilution of 1:1000. Anti-β-COP antibodies raised in rabbits (1:200) were a kind gift of Tom Wileman (University of East Anglia). Anti-β-Actin mouse antibodies (1:200) were purchased from Sigma. WGA conjugated to Alexa-Fluor 555 was from Molecular probes (Invitrogen). Secondary Alexa-Fluor 488 conjugate goat anti-rabbit IgG antibodies and Alexa-Fluor 546 goat conjugate anti-mouse antibodies were used at a dilution of 1:500 and purchased from Molecular probes (Invitrogen).

4.2.2 Preparation of cells BHK-21 cells for Immunofluorescence

Cells were grown on sterile 13 mm glass coverslips in a 6-well plate and infected as described in section 3.2.7. The cells were fixed at various times post-infection. The medium was removed and the cells washed with PBS. Coverslips were transferred into the wells of a 24-well plate for immunofluorescence staining. Cells were fixed with ice-cold methanol and air-dried prior to dual-labelling with WGA and anti-β-COP antibodies or anti-TMEV 2C antibodies and anti-β-actin antibodies. Because the signal for anti-β-COP was stronger when cells were fixed with paraformaldehyde, this was used for single labelling with anti-β-COP antibodies. Cells were fixed in 4% paraformaldehyde for 20 min at RT.

4.2.3 Indirect immunofluorescence staining of infected cells

WGA was prepared as 1 mg/ml stock in PB and stored at -20°C. When used as a stain, the stock was thawed on ice and diluted 1:250 in blocking solution (PB containing 2 % BSA) and allowed to stain the cells for 20 min at RT, and then at 37°C for 10 min. Cells were then permeabilised, blocked and subjected to indirect immunofluorescence staining essentially as described in section 3.2.8. Bound anti-β-COP antibodies were detected with Alexa-Fluor 488-conjugated secondary antibodies. WGA is conjugated to Alexa-Fluor 546. Cells were imaged as described in section 3.2.9. Optical sectioning was performed by collecting five triple-labelled, 8-bit images at 1 μm intervals in a Z-stack.

4.3 Results and discussion

4.3.1 Localisation of β-COP and WGA in uninfected cells

The first experiment was performed in order to investigate whether WGA could be used as a Golgi marker to determine the localisation of 2C protein. WGA is a lectin which binds sialic acid residues on glycoproteins (Wright, 1984) and has been widely used to study membrane trafficking pathways in cells (Allen *et al.,* 1989; Balin & Broadwell, 1987; Mezitis *et al.,* 1987; Rhodes *et al.,* 1986). Intracellular binding of WGA is mainly concentrated in the membranes of organelles located distally in protein trafficking pathways, specifically endosomes, lysosomes and the Golgi apparatus (Hedman *et al.*, 1986). β-COP is a 110 kDa protein found in the peripheral region of the Golgi (Duden *et al.*, 1991). Uninfected cells were fixed in methanol and co-stained with WGA and antibodies against β-COP. The images obtained by confocal microscopy are shown in Figure 4.1.

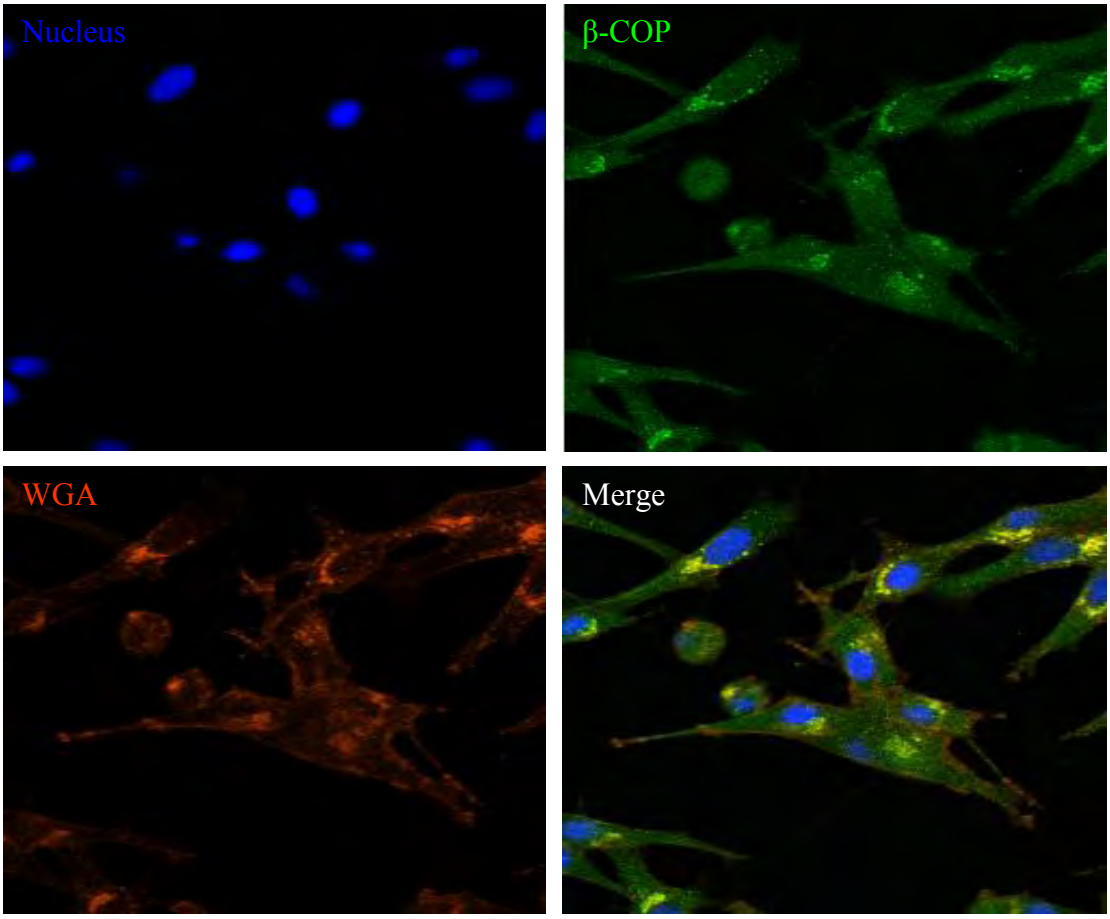

Figure 4.1: Localisation of β-COP with WGA in uninfected BHK-21 cells. Cells grown on coverslips were fixed with ice-cold methanol and stained with WGA followed by permeabilisation and immunostaining with anti-β-COP antibodies. Primary antibodies were detected with Alexa-Fluor 488-conjugated goat anti-rabbit antibodies. WGA is conjugated to Alexa-Fluor 555.

Figure 4.1 clearly shows that the signals for WGA and β-COP overlap. The bright signal for WGA (bottom left) is seen concentrated in the perinuclear region with faint cytoplasmic and plasma membrane staining. The Golgi apparatus is composed of a set of closely stacked cisternae and associated vesicles, and mediates transport from ER to the cell surface (Torrisi & Pinto, 1984). The secretory pathway allows soluble and membrane proteins to be transported from the ER through the Golgi complex where they are glycosylated, and to various locations including lysosomes, endosomes, secretory vesicles, and the plasma membrane (Duden *et al.*, 1991). As described in the introduction to this chapter, WGA is a lectin which binds carbohydrate residues on glycoproteins. This explains why, when applied to cells, the stain is distributed predominantly in the perinuclear region where the Golgi apparatus is situated, and also on cytoplasmic vesicles and the plasma membrane (Figure 4.1, bottom left panel). As expected, β-COP, which stains the peripheral Golgi area (Knox *et al.*, 2005; Monaghan *et al.*, 2004) is localised only in the perinuclear region (top right). The merged image shows that the two signals overlap in the region of the Golgi apparatus and the yellow colour suggests co-localisation. These results indicated that WGA can be used to stain the Golgi apparatus. The next experiment was to investigate whether 2C protein could be co-localised with WGA which would test the hypothesis that the viral protein targets the Golgi apparatus.

4.3.2 Localisation of 2C protein to the Golgi apparatus using WGA

Studies with FMDV have shown that replication complexes containing viral proteins are found in the perinuclear region close to the Golgi complex (Dales et al., 1965). In addition, early studies demonstrated large membrane vesicles forming in the perinuclear region in close proximity to the Golgi apparatus in PV-infected cells (Garcia-Briones *et al.,* 2006; Knox *et al.,* 2005). To determine whether TMEV also targets the Golgi complex, cells grown on coverslips were infected with TMEV and fixed at 5 hpi with methanol. The cells were stained with WGA, permeabilised, incubated with anti-TMEV 2C antibodies, and examined by confocal microscopy.

Figure 4.2 (Panel A) shows WGA concentrated to one side of the nucleus with some cytoplasmic and plasma membrane staining. 2C protein is distributed in the cytoplasm and, in most cells, concentrated on one side of the nucleus (panel B). The two signals

overlap extensively in the merged image as seen in panel C. Interestingly, the marked region (X) in panel A seems to be devoid of the stain, while in panel B this region is occupied by the 2C protein signal (Y). The yellow colour (Z) in the merged image indicates partial co-localisation between WGA and 2C protein signals suggesting that the virus is targeting Golgi membranes.

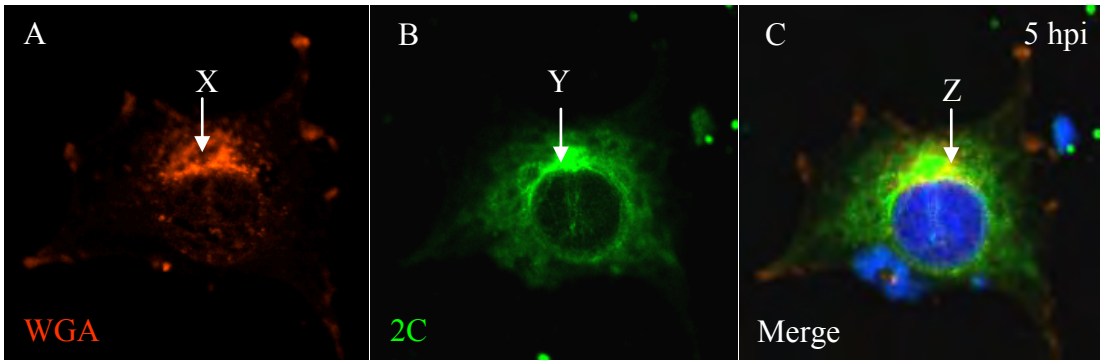

Figure: 4.2: Localisation of 2C protein to the Golgi apparatus using WGA. Cells were infected with TMEV and allowed to express viral proteins for 5 hours. The cells were then fixed in methanol and stained with WGA (Panel A) and anti-TMEV 2C antibodies (Panel B). Panel C is the merged image. Alexa-Fluor 488-conjugated goat anti-rabbit antibodies were used to detect the anti-TMEV 2C antibodies.

To further analyse co-localisation between 2C protein and WGA, optical sectioning was performed and a Z-stack obtained. Each section gives information about the relationship between signals and determines whether the signals co-localise when the different channels are superimposed. Optical slices were collected at 1 µm intervals in a Z-stack. Figure 4.3 is a gallery of five consecutive optical sections of infected cells with the different channels (orange, green and blue) superimposed.

In all sections, the 2C protein signal is concentrated to one side of the nucleus. The WGA signal is not strong and is distributed in the cytoplasm and in the perinuclear region where 2C protein is located. However, what is interesting about these images is that in the region of overlap, green (2C protein) and red (WGA) appear to be mostly separate and there is very little visible yellow colouring. This observation could mean that, although the distribution of 2C protein overlaps with the Golgi marker and is targeted to Golgi membranes, the two signals do not co-localise. Interestingly, this observation is consistent with that made for FMDV in experiments using fluorescence microscopy and digital deconvolution (Knox *et al.*, 2005). It was found that, although

FMDV 2C protein locates to the Golgi apparatus and overlaps with the distribution of the Golgi marker mannosidase II, there was no co-localisation of the two signals. It was concluded that replication sites forms in the region of the Golgi apparatus but exclude host marker proteins by some unknown mechanism.

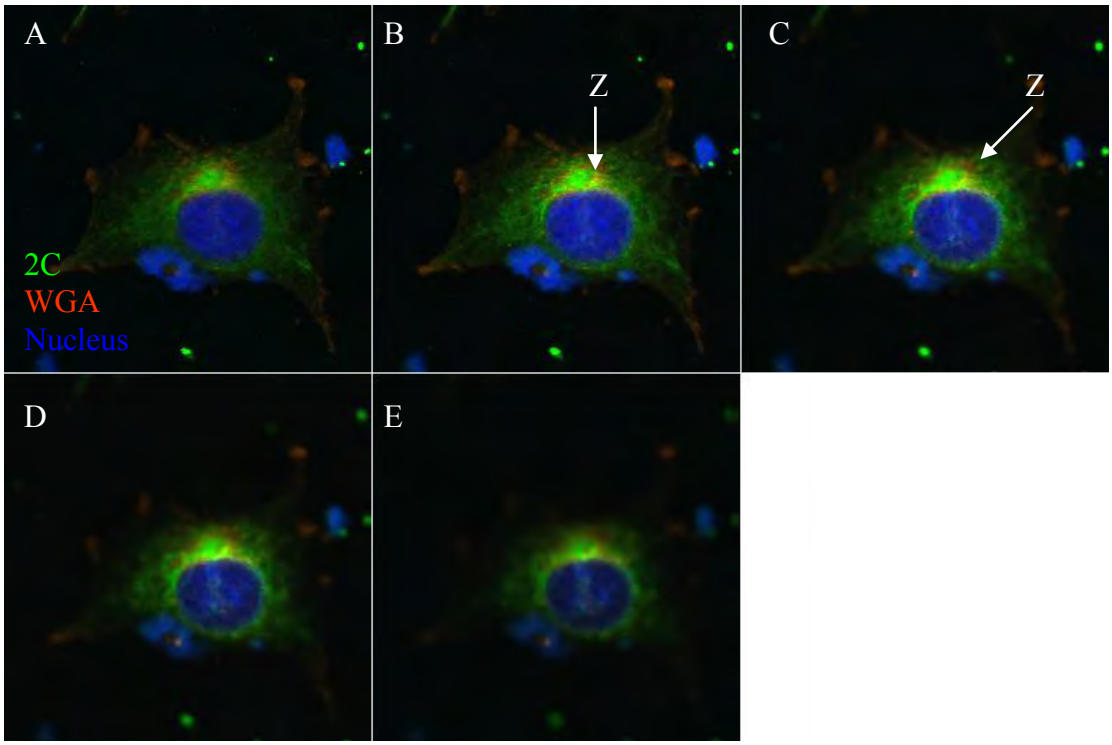

Figure 4.3: Optical sectioning of a TMEV-infected cell. Infected cells fixed 5 hpi were stained with WGA and anti-TMEV 2C antibodies. Alexa-Fluor 488-conjugated goat anti-rabbit antibodies were used to detect 2C antibodies. Panels A-E represents 5 optical sections captured at 1µm intervals. Arrowhead Z represents possible co-localisation between the two signals (yellow).

Moreover, this and another study showed that FMDV 2C protein does not co-fractionate with Golgi markers suggesting that the Golgi complex is not a source of structures containing 2C protein (Bienz *et al.*, 1987; Rust *et al.*, 2001). Further experiments are needed to confirm this observation for TMEV 2C protein, but the present results suggest that the virus behaves like FMDV in that it utilises Golgi membranes for its replication but excludes host proteins in the process. In panel B and C (arrowhead Z) there appears to be some yellow colouring that may represent partial co-localisation. Alternatively, and more likely, the yellow colour may be as a result of over-exposure of one or both of the signals. To conclusively determine whether the two signals co-localise, optical sections can be analysed using Image J software to

obtain correlation data. However, many sections would require analysis and due to time constraints, this was not performed in this study.

4.3.3 Effect of TMEV infection on Golgi distribution

The numerous membrane vesicles that accumulate in the cytoplasm of picornavirus-infected cells are thought to be derived from the Golgi complex and ER (Sandoval & Carrasco, 1997; Schlegel *et al.*, 1996). It has also been demonstrated that, during PV infection, the Golgi complex disassembles (Duden *et al.*, 1991).To determine whether TMEV infection causes a change in Golgi structure, the distribution of β-COP alone was examined at various times post-infection. Cells growing on coverslips were infected with TMEV and fixed with paraformaldehyde at 0, 2, and 8 hpi. Figure 4.4 shows images obtained by confocal microscopy.

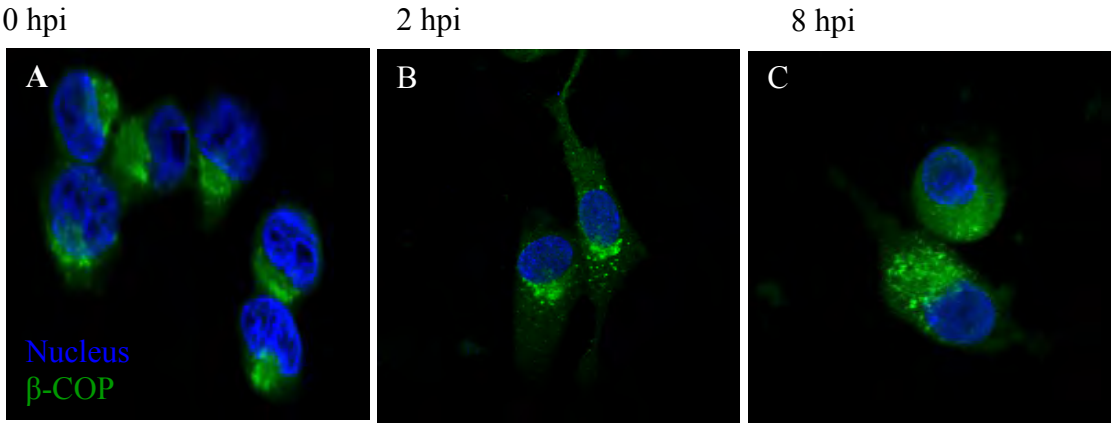

Figure 4.4: Changes in β-COP distribution during TMEV infection. Infected **c**ells were fixed with paraformaldehyde at 0 hpi (Panel A), 2 hpi (Panel B) and 8 hpi (Panel C) and stained with anti-β-COP antibodies. These were detected with Alexa-Fluor 488-conjugated goat anti- rabbit antibodies.

Figure 4.4 shows that the distribution of β-COP changes as infection progresses (compare panels A and C). Panel A shows a compact crescent-shaped Golgi organisation in uninfected cells at 0 hpi. β-COP staining is still concentrated in the perinuclear region 2 hpi, but some dispersal of the signal is apparent (Panel B). At 8 hpi (Panel C), the Golgi complex has formed a round-shaped structure and the β-COP signal is observed throughout the cytoplasm. The diffuse staining in panel C suggests that TMEV causes a change in the structural organisation of the Golgi complex as was shown for FMDV (Knox *et al.*, 2005; Monaghan *et al.*, 2004)

4.3.4 Time course of WGA distribution during TMEV infection

It is clear from Figure 4.3 that the distribution of WGA is not as prominent in the Golgi area as in uninfected cells. This observation was made in the majority of infected cells (data not shown). To investigate whether there is a change in the distribution of WGA over time as was observed for β-COP, infected cells were fixed with methanol at 6, 7 and 8 hpi, double-stained with WGA and anti-TMEV-2C antibodies and examined by confocal microscopy [(Figure 4.5 (I)]. Cells were not analysed at 2 and 4. At 6 hpi (panel A) the stain appears to have a cytoplasmic distribution and bright signals are observed in the region of the Golgi complex and on the plasma membrane as expected. 2C protein is present at this stage both in the cytoplasm and in the perinuclear region (panel B). In the merged image, the two signals overlap as was observed in previous experiments.

In a parallel experiment, expression of 2C protein was analysed over time in infected cells by Western blotting to determine at what time point the 2C protein signal appeared. Cells were infected in four 25 cm^2 flasks, collected at 2, 4, 6 and 8 hpi, and resuspended in lysis buffer. Total cell lysates were analysed by SDS-PAGE and Western blotting using anti-TMEV 2C antibodies. In Figure 4.5 (II), lane 2 and 3 clearly show that the protein is not expressed until 6 hpi consistent with immunofluorescence analysis results which showed the 2C protein signal at 6 hpi distributed in the cytoplasm. It is possible that the protein was present at 5 hpi but the cells were not analysed at that point. These results together with the results in Figure 4.2 (panel B), suggest that 5 and 6 hours can be regarded as early stages of infection where the 2C protein signal is observed in the cytoplasm and in the perinuclear region. The 8 hour time point represents late infection and 2C protein is found in a large structure to one side of the nucleus and overlapping the Golgi apparatus (panel C). These results correlate with those observed in Figure 4.5 (II) where more of the protein is present at 8 hpi compared to 6 hpi (compare lanes 3 and 4).

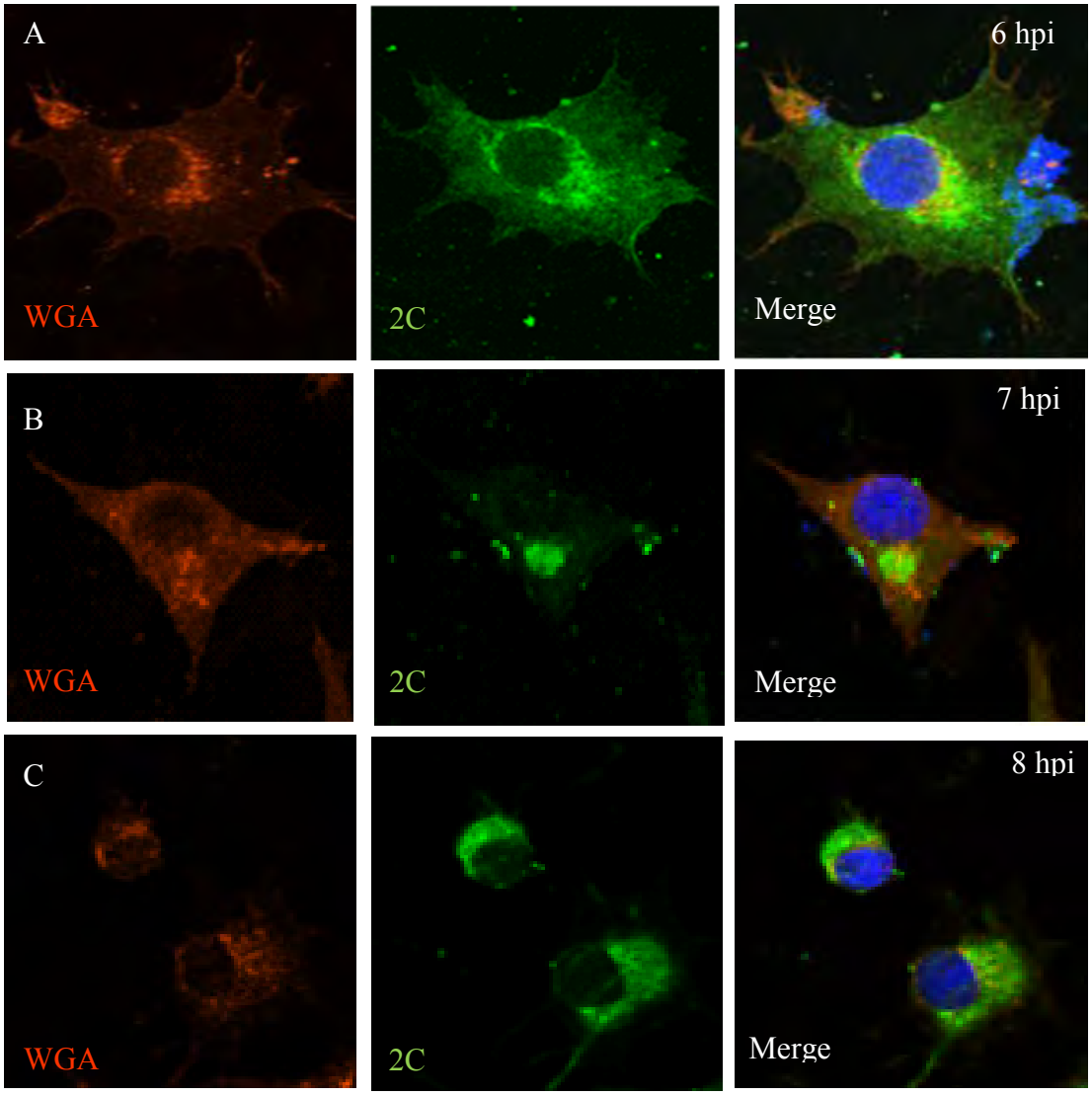

Figure 4.5 (I): Time course of the distribution of WGA relative to 2C protein in infected cells. Cells were infected and fixed with methanol at 6, 7 and 8 hpi. 2C protein was localised with anti-TMEV 2C antibodies (green) and the Golgi with WGA (orange). Alexa-Fluor 488-conjugated goat anti-rabbit antibodies were used to visualise primary anti-TMEV 2C antibodies.

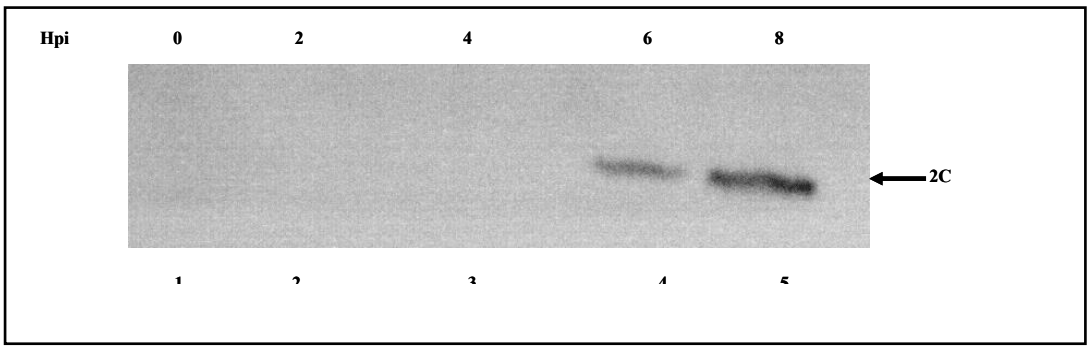

Figure 4.5 (II): Western Blot analysis of the expression of TMEV 2C protein in infected BHK-21 lysate over time. Lane 1: Uninfected, Lanes 2-5: lysate analysed at 2, 4, 6 and 8 hpi. Primary anti-TMEV 2C antibodies were used at 1:10000 dilution.

The distribution of WGA at 7 hpi [Figure 4.5 (I)], (Panel B) appears to have changed slightly with stronger cytoplasmic staining and less concentration in the perinuclear region. The 2C protein signal has now become concentrated on one side of the nucleus. At 8 hpi (Panel C), the cells are showing signs of rounding up and the signal for WGA is no longer concentrated in the perinuclear region, but is distributed throughout the cell. The signal for WGA was also found to be weak at this time point and it was difficult to obtain clear images. 2C protein, however, was present in a large structure adjacent to the nucleus and staining was intense. These results are consistent with the previous experiment showing a redistribution of β-COP, and suggest that TMEV indeed induces a change in Golgi structure during infection. It is worthwhile to note the change in the cell shape as infection progresses. Positive-strand RNA viruses are known to induce CPE during infection and eventually lyse their host cells. The cells were initially flat and attached to the growth surface before and during early infection. At later stages, they tended to round up and detach from the surface. These effects were examined in the next experiments.

4.3.5 Morphological changes and distribution of β-actin in TMEV-infected cells

The cell cytoskeleton is a dynamic structure within the cytoplasm which is responsible for maintenance of cell shape, intracellular trafficking and cell division (Bedows *et al.,* 1983; Hollinshead *et al.,* 2001; Jouvenet & Wileman, 2005; Sandoval & Carrasco, 1997). It is composed of three components namely, actin filaments, intermediate filaments, and microtubules. The actin filaments together with microtubules are known to be involved in virus entry, replication and release (Fernie & Gerin, 1982; Kallewaarda *et al.,* 2005). Viruses, in general, use and modify the cytoskeleton during infection and this is well documented (Bedows *et al.,* 1983; Hollinshead *et al.,* 2001; Jouvenet & Wileman, 2005; Ploubidou *et al.,* 2000; Zhai *et al.,* 1988). Picornaviruses are also known to use and re-structure the cytoskeleton for attachment, entry, replication and release of the virions (Langford, 1995). TMEV is associated with intermediate filaments in infected cells (Nédellec *et al.,* 1998) and FMDV infection results in collapse of microtubules around the replication complex (Armer *et al.,* 2008; Monaghan *et al.,* 2004). PV also affects the cytoskeleton by inducing structural changes in a microtubule-associated protein (Joachims & Etchison, 1992; Lenk & Penman, 1979). It was apparent in previous experiments that

TMEV induces a change in cell morphology during infection. To examine if this is related to changes in the cytoskeleton, the distribution of β-actin during infection was investigated in infected cells. Cells were infected with TMEV and fixed with methanol at 0, 6 and 8 hpi. Anti-β-actin antibodies were detected using Alexa-Fluor 546-conjugated mouse antibodies. The cells were co-stained with anti-TMEV 2C antibodies and these were detected with Alexa-Fluor 488-conjugated rabbit antibodies (Figure 4.6).

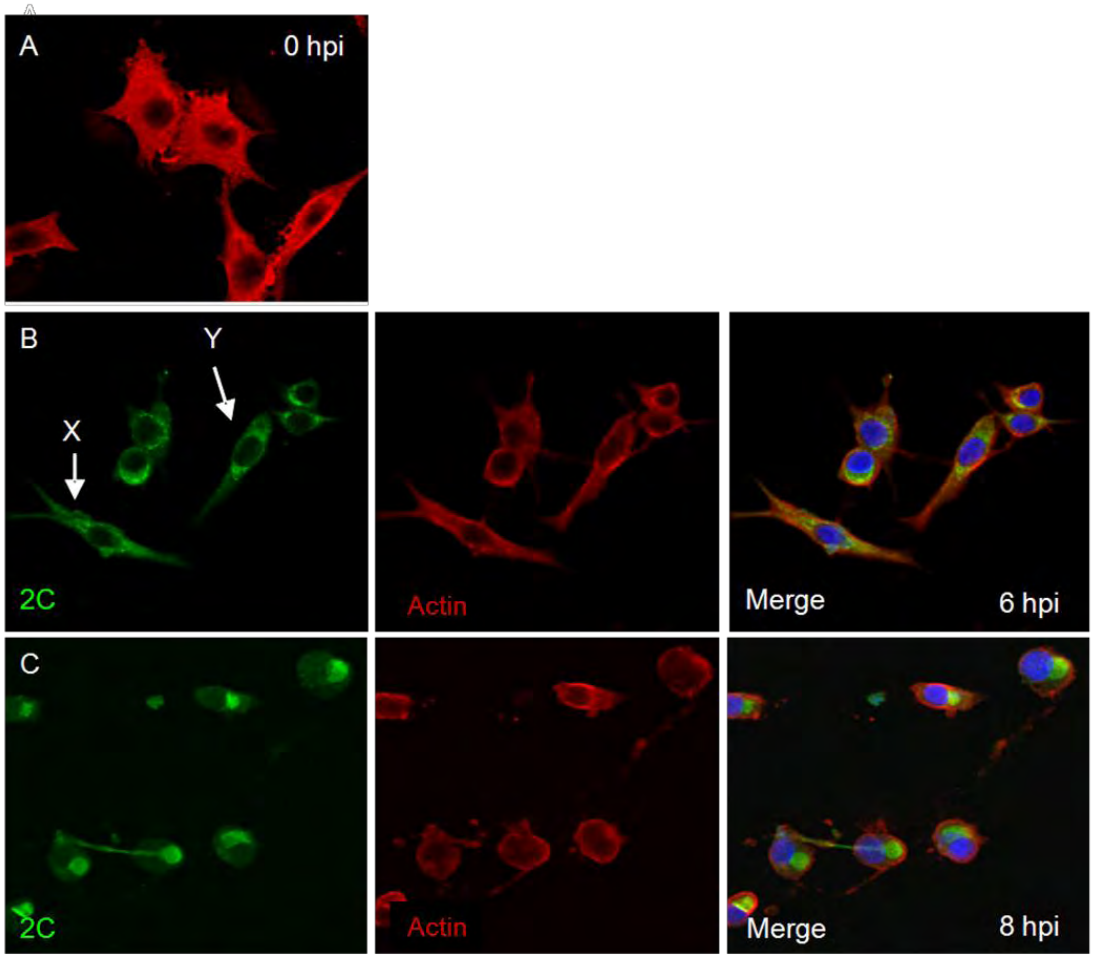

Figure 4.6: Distribution of β-actin during TMEV infection. Infected cells were fixed with methanol at 0 hpi (panel A), 6 hpi (Panel B) and 8 hpi (Panel C). The cells were double labelled with anti-β-Actin antibodies and anti-TMEV 2C antibodies which were detected with Alexa-Fluor 546-conjugated goat anti-mouse and Alexa-Fluor 488-conjugated goat anti-rabbit antibodies respectively.

Panel A shows the distribution of β-actin in uninfected cells. The protein is distributed in a reticular pattern throughout the cell cytoplasm and is absent from the nucleus. At 6 hpi (Panel B), 2C protein staining is evident. At this stage, some cells still show their typical fibroblast shape (arrowhead X) and β-actin staining is mainly cytoplasmic as in uninfected cells. However, many cells have begun to round up

(arrowhead Y) and β-actin appears to be concentrated towards the outer edges of the cells. At 8 hpi (Panel C), 2C protein containing structures occupy almost 50% of cell volume, and β-actin is seen as a ring around the nucleus and replication complex. These results show that TMEV behaves similarly to PV and FMDV in that cytoskeletal changes associated with CPE are induced at late stages of infection.

4.4 Conclusions

The main aim of the experiments described in this chapter was to localise TMEV 2C protein in infected cells and to determine the effects of infection on Golgi and cytoskeletal structure. WGA was chosen as a Golgi stain since we could not use the anti-β-COP antibodies available in the laboratory at the same time with the anti-TMEV 2C antibodies. It was shown that WGA can be used to stain the Golgi complex because there was extensive overlap and potential co-localisation between the stain and β-COP. Golgi elements were rearranged by TMEV as suggested by dispersal and fading of WGA and β-COP signals during infection. The 2C protein and WGA signals also overlapped extensively, suggesting that the virus targets the Golgi apparatus. Although optical sectioning revealed that the two signals remained separate in the merged image, further analysis is required to conclude whether they co-localise or not. The localisation of the 2C protein appears to vary during infection. At early stages it was observed in the cytoplasm and in the perinuclear region, and with prolonged infection, 2C protein was located in one large structure comprising almost 50% of cell volume. The cell cytoskeleton was disrupted during infection as indicated by a change in β-actin staining during infection. In uninfected cells it appears as a network throughout the cytoplasm. Late in infection, β-actin had formed a shell around the nucleus and the replication complex.

5. General conclusions and future work

This study sought to generate polyclonal antibodies against TMEV 2C protein for use in localisation of the protein in infected cells. Picornavirus 2C proteins are known to bind membranes and therefore may be potentially insoluble when expressed in a bacterial system. Thus, a bioinformatic analyses was performed on the TMEV 2C protein amino acid sequence to identify regions with predicted hydrophilic and antigenic properties. Based on the results of these analyses, a region of the 2C protein (amino acids 31-210) was selected for expression and purification to prepare antibodies. Nucleotides corresponding to the selected region of 2C protein were PCR-amplified and cloned into pQE-80L for expression in *E. coli* cells by IPTG induction. The peptide was found to be maximally expressed at 5 hours post-induction although in an insoluble form. Treatment of cell lysates with sarcosyl solubilised some of the peptide. Culture volume was upscaled to obtain sufficient antigen for the immunisation of rabbits. From this upscaled culture, 1.5 mg of peptide was purified using Ni-NTA affinity chromatography and used for antibody production.

Rabbit anti-serum (anti-TMEV 2C antibodies) was tested for specificity and sensitivity using bacterially-expressed 2C peptides, and was found to be highly specific for both the antigen, 2C (31-210) and also 2C (31-326) which are truncated forms of the full-length 2C protein. Furthermore, the anti-TMEV 2C antibodies were able to detect virally-expressed 2C protein in infected cells. The full-length protein was recovered in the supernatant and pellet fractions indicating that the protein is both soluble in the cytoplasm and membrane-bound.

Preliminary testing of the antibodies on infected cells by immunofluorescence analysis showed two stages of infection as the cells examined displayed different 2C protein staining. In some cells, the distribution of the 2C protein was cytoplasmic and perinuclear, while in other cells, it was seen in one large structure next to the nucleus resembling a Golgi distribution. It could be argued that, as demonstrated for FMDV 2C protein, a diffuse cytoplasmic distribution represents an early stage of infection while the other distribution is characteristic of late infection. The localisation of

TMEV 2C protein next to the nucleus prompted the next experiment which sought to investigate whether the protein was targeting the Golgi apparatus. Since the Anti-β-COP antibodies could not be used in dual labelling experiments with the anti-TMEV 2C antibodies; WGA was used as a marker for the Golgi as it had been shown in previous studies to bind membranes of organelles involved in protein trafficking pathways, specifically endosomes, lysosomes and the Golgi apparatus. WGA was tested for its ability to stain the Golgi apparatus by dual-immunolabelling with anti-β-COP antibodies in uninfected cells. Total overlap between the signals was observed in the perinuclear region. It was also observed that WGA was distributed in the cytoplasm and on the plasma membrane. Since WGA was effective in staining the Golgi apparatus, the next experiment was aimed at localising 2C protein to the Golgi using WGA. Dual-labelling studies using WGA and anti-TMEV 2C antibodies revealed that the two signals overlapped in the Golgi region. It is interesting to note (refer Figure 4.3.2) that, although the two signals overlapped and were found in the same region, there was a large region that the anti-TMEV 2C antibodies stained which the WGA did not (shown by the X in the figure). In order to investigate the nature of this partial overlap, optical sectioning was performed and a Z-stack obtained. The results showed that the two signals overlapped but remained separated to a large degree. More studies are needed to confirm if in fact 2C protein and WGA co-localise. It was seen by examining the distribution of β-COP and WGA that the Golgi apparatus reorganises during infection and the changes become more apparent as infection progresses. This may be due to the fact that picornaviruses use host cell membranes to form the vesicles on which replication occurs, and Golgi membranes are used in this process.

It was further observed during this study that infected cells displayed a change in morphology as infection progressed. The cells tended to "round up" during late infection and lost their ability to attach to growth surface. In order to show and monitor this effect, β-actin antibodies were used to stain infected cells. The distribution of β-actin changed during infection from a reticular staining to one that was concentrated in a ring around the viral replication complex containing 2C protein.

The synthesis of anti-TMEV 2C antibodies has opened new doors in terms of the experiments that can be performed in the future. With this antibody, membrane

association properties of TMEV 2C and 2BC viral proteins can be investigated. These investigations will involve transient expression of the proteins and co-immunoprecipitation with various host cells organelle marker. The effects of infection on the ultra-structure of cells can also be investigated using this antibody by transmission electron microscopy. These antibodies can also help elucidate whether TMEV 2C and/or 2BC proteins induce the disassembly of the Golgi complex or takes part in the formation of vesicles as has been shown for other piconaviruses. A transport assay can also be conducted to determine whether these proteins are involved in the disruption of protein trafficking through the exocytic pathway. Finally, other future studies involving these antibodies will investigate interactions between 2C protein and host cell proteins using biochemical and *in vivo* techniques. Identification of such interactions could lead to the development of anti-viral agents that target picornavirus replication.

REFERENCES

Agol, V. I. (2002). *Picornavirus genome: an overview. In Molecular Biology of Picornaviruses* Washington D.C., USA ASM Press.

Agudelo, P., Botero, D. & Palacio, L. G. (2005). Evaluation of the ELISA method for diagnosis of human cysticercosis in an endemic region. *Biomedica* **25**, 488-495.

Aldabe, R. & Carrasco, L. (1995). Induction of Membrane Proliferation by Poliovirus Protein 2C and 2BC. *Biochemical and Biophysical Research Communications* **206**, 64-76.

Allen, R. D., Schroeder, C. C. & Fok, A. K. (1989). Intracellular Binding of Wheat Germ Agglutinin by Golgi Complexes, Phagosomes, and Lysosomes of *Paramecium multimicronucleatum*. *J Histochem Cytochem* **37**, 195-202.

Anasetti, C., Hansen, J. A., Waldmann, T. A., Appelbaum, F. R., Davis, J., Deeg, H. J., Doney, K., Martin, P. J., Nash, R., Storb, R., Sullivan, K. M., Witherspoon, R. P., Binger, M. H., Chizzonite, R., Hakimi, J., Mould, D., Satoh, H. & Light, S. E. (1994). Treatment of Acute Graft-Versus-Host Disease With Humanized Anti-Tac: An Antibody That Binds to the Interleukin-2 Receptor. *Blood* **84**, 1320-1327.

Argos, P., Krammer, G., Nicklin, M. J. H. & Wimmer, E. (1984). Similarity in gene organization and homology between proteins of animal picornaviruses and plant comovirus suggest a common ancestry of these virus families. *Nucleic Acids Res* **12**, 7251-7267.

Arita, I., Nakane, M. & Fenner, F. (2006). Is Polio Eradication Realistic. In Science*: Topics in Virology*

Armer, H., Moffat, K., Wileman, T., Belsham, G. J., Jackson, T., Duprex, W. P., Ryan, M. & Monaghan, P. (2008). Foot-and-Mouth Disease Virus, but Not Bovine Enterovirus, Targets the Host Cell Cytoskeleton via the Nonstructural Protein $3C^{pro}$. *J Virol* **82**.

Balin, B. J. & Broadwell, R. D. (1987). Lectin-labeled membrane is transferred to the Golgi complex in mouse pituitary cells *in vivo*. *J Histochem Cytochem* **35**, 489-498.

Banerjee, R., Echeverri, A. & Dasgupta, A. (1997). Poliovirus-Encoded 2C Polypeptide Specifically Binds to the 3'-Terminal Sequences of Viral Negative-Strand RNA. *J Virol* **71**, 9570-9578.

Banerjee, R. & Dasgupta, A. (2001). Interaction of picornavirus 2C polypeptide with the viral negative-strand RNA. *J Gen Virol* **82**, 2621-2627.

Banerjee, R., Tsai, W., Kim, W. & Dasgupta, A. (2001). Interaction of Poliovirus-Encoded 2C/2BC Polypeptides with the 3' Terminus Negative-Strand Cloverleaf Requires an Intact Stem-Loop b. *Virol* **280**, 41-51.

Banerjee, R., Weidman, M. K., Echeverri, A., Kundu, P. & Dasgupta, A. (2004). Regulation of Poliovirus 3C Protease by the 2C Polypeptide. *J Virol* **78**, 9243-9256.

Baran, J., Pituch-Noworolska, A., Krzeszowiak, A., Wieckiewicz, J., Stachura, J., Pryjma, J., Popiela, T., Szczepanik, A. & Zembala, M. (1998). Detection of cancer cells in the blood by FACS sorting of CD45- cells. *Int J Mol Med* **1**, 573-578.

Barteling, S. J. (2004). Modern inactivated Foot-and-mouth disease (FMD) vaccines: historical background and key elements in production and use. In *Foot and*

Mouth Disease: Current Persectives. Edited by F. S. Domingo. Norfolk: Horizon Bioscience.

Bedard, K. M. & Semler, B. L. (2004). Regulation of picornavirus gene expression. *Microbes and Infection* **6**, 702-713.

Bedows, E., Rao, K. M. & Welsh, M. J. (1983). Fate of microfilaments in Vero cells infected with measles virus and herpes simplex virus type 1. *Mol Cell Biol* **3**, 712-719.

Belsham, G. J. & Brangwyn., J. K. (1990). A region of the 5' noncoding region of foot-and-mouth disease virus RNA directs efficient internal initiation of protein synthesis within cells: involvement with the role of L protease in translational control. *J Virol* **64**: 11, 5389-5395.

Bernstein, H., Sarnow, P. & Baltimore, D. (1986). Genetic complementation among poliovirus mutants derived from an infectious cDNA clone. *J Virol* **60**, 1040-1049.

Bienz, K., Egger, D., Rasser, Y. & Bossart, W. (1983). Intracellular distribution of poliovirus proteins and the induction of virus-specific cytoplasmic structures. *Virol* **131**, 39-48.

Bienz, K., Egger, D., Rasser, Y. & Loeffler, H. (1987). Association of polioviral proteins of the P2 genomic region with the viral replication complex and virus-induced membrane synthesis as visualised by electron microscopic immunocytochemistry and autoradiography. *Virol* **160**, 220-226.

Bienz, K., Egger, D., Troxler, M. & Pasamontes, L. (1990). Structural Organization of Poliovirus RNA Replication Is Mediated by Viral Proteins of the P2 Genomic Region. *J Virol* **64**, 1156-1163.

Bienz, K., Egger, D., Pfister, T. & Trolex, M. (1992). Structural and Functional Characterisation of the Poliovirus Replication Complex. *J Virol* **66**, 2740-2747.

Bonifacino, J. S., Dell'Angelica, E. C. & Springer, T. A. (2001). Immunoprecipitation. In *Current Protocols in Immunology*, pp. 8.3.1-8.3.28. Edited by J. E. Coligan, A. M. Kruisbeek, D. H. Margulies, E. M. Shevach & W. Strober. New York John Wiley and Sons, Inc.

Bumgardner, G. L., Hardie, I., Johnson, R. W., Lin, A., Nashan, B., Pescovitz, M. D., Ramos, E. & Vincenti, F. (2001). Phase III Daclizumab Study Group: Results of 3-year phase III clinical trials with daclizumab prophylaxis for prevention of acute rejection after renal transplantation. *Transplantation* **15**, 839-845.

Caliguiri, L. A. & Tamm, I. (1969). Membranous structures associated with translation and transcription of poliovirus RNA. *Science* **166**, 885-886.

Caliguiri, L. A. & Tamm, I. (1970). The role of cytoplasmic membranes in poliovirus biosynthesis. *Virol* **42**, 100-111.

Cann, A. J. (2005). *Principles of Molecular Virology*. University of Leicester, UK.

Cao, Y. Z., Valentine, F., Hojvat, S., Allain, J. P., Rubinstein, P., Mirabile, M., Czelusniak, S., Leuther, M., Baker, L. & Friedman-Kien, A. E. (1987). Detection of HIV antigen and specific antibodies to HIV core and envelope proteins in sera of patients with HIV infection. *Blood* **70**, 575-578.

Carrasco, L., Guinea, R., Irurzun, A. & Barco, A. (2002). Effects of viral replication on cellular membrane metabolism and function. *In Molecular Biology of Picornaviruses*, pp. 337-354. Edited by B. L. Semler & E. Wimmer. Washington D.C,USA: ASM Press.

Carrasco, L. & Smith, A. E. (1976). Sodium ions and the shut-off of host cell protein synthesis by picornaviruses. *Nature* **264**, 807-809.

Carter, P. (2001). Improving the efficacy of antibody-based cancer therapies. *Nat Rev Cancer* **1**, 118-129.

Cho, M. W., Teterina, N., Egge, D., Bienz, K. & Ehrenfeld, E. (1994). Membrane rearrangement and vesicle induction by recombinant poliovirus 2C and 2BC in human cells. *Virol* **202**, 129-145.

Coico, R., Sunshine, G. & Benjamin, E. (2003). *Immunology. A short course* John Wiley & Sons.

Costa-Mattioli, M., Napoli, A. D., Ferré, V., Billaudel, S., Perez-Bercoff, R. & Juan, C. (2002). Genetic variability of hepatitis A virus. *J Gen Virol* **84** 3191-3201.

Crawford, N. M. & Baltimore, D. (1983). Genome-linked protein VPg of poliovirus is present as free VPg and VPg-pUpU in poliovirus-infected cells. *Proc Natl Acad Sci* **80**, 7452-7455.

Dales, S., Eggers, H. J., Tamm, I. & Palade, G. E. (1965). Electron microscopic study of the formation of poliovirus. *Virol* **26**, 379-389.

de Jong, A. S., Wessels, E., Dijkman, H. B. P. M., Galama, J. M. D., Melchers, W. J. G., Willems, P. H. G. M. & Kuppeveld, F. J. M. v. (2003). Determinants for Membrane Association and Permeabilization of the Coxsackievirus 2B Protein and the Identification of the Golgi Complex as the Target Organelle. *J Biol Chem* **278**, 1012-1021.

de Jong, A. S. F., Mattia, F. D., van Dommelen, M. M., Lanke, K., Melchers, W. J. G., Willems, P. H. G. M. & van Kuppeveld, F. J. M. (2008). Functional Analysis of Picornavirus 2B Proteins: Effects on Calcium Homeostasis and Intracellular Protein Trafficking. *J Virol* 82:3782-3790.

de Soet, J. J., van Dalen, P. J., Russell, R. R. B. & de Graaff, J. (1990). Identification of mutans streptococci with monoclonal antibodies. *Antonie van Leeuwenhoek* **58**, 219-225.

Devaney, M. A., Vakharia, V. N., Lloyd, R. E., Ehrenfeld, E. & Grubman, M. J. (1988). Leader protein of foot-and-mouth disease virus is required for cleavage of the p220 component of the cap-binding protein complex. *J Virol* **62**, 4407-4409.

Doedens, J. R. & Kirkegaard, K. (1995). Inhibition of cellular protein secretion by poliovirus proteins 2B and 3A. *EMBO Journal* **14**, 894-907.

Doedens, J. R., Jr. Giddings, T. H. & Kirkegaard, K. (1997). Inhibition of endoplasmic reticulum-to-Golgi traffic by poliovirus protein 3A: genetic and ultrastructural analysis. *J Virol* **71**, 9054-9064.

Domingo, E. & Holland, J. J. (1997). RNA virus mutations and fitness for survival. *Ann Rev Microbiol* **51**, 151-178.

Donnelly, M. L. L., Gani, D., Flint, M., Monaghan, S. & Ryan, M. D. (1997). The cleavage activities of apthovirus and cardiovirus 2A proteins. *J Gen Virol* **78**, 13–21.

Duden, R., Griffiths, G., Frank, R., Argos, P. & Kreis, T. E. (1991). B-COP, a protein associated with non-clathrin coated vesicles and the Golgi complex shows homology to B-adaptin. *Cell* **64**, 649-665.

Echeverri, A., Banerjee, R. & Dasgupta, A. (1998). Amino-terminal region of poliovirus 2C protein is sufficient for membrane binding. *Virus Research* **54**, 217-223.

Echeverri, A. & Dasgupta, A. (1995). Amino terminal regions of poliovirus 2C protein mediate membrane binding. *Viroy* **208**, 540-553.

Emini, E. A., Schleif, W. A., Colonno, R. J. & Wimmer, E. (1985). Antigenic conservation and divergence between the viral-specific proteins of poliovirus type 1 and various picornaviruses. *Virol* **140**, 13-20.

Flanegan, J. B. & Baltimore, D. (1977). Poliovirus-specific primer-dependent RNA polymerase able to copy poly (A). *Proc Natl Acad Sci* **74**, 3677-3680.

Flint, S. J., Enquist, L. W., Racaniello, V. R. & Skalka, A. M. (2004). *Principles of Virology: Molecular Biology, Pathogenesis, and Control of animal Viruses*. Washington, DC: ASM Press.

Fox, J. P. (1976). Is a rhinovirus vaccine possible? *American J Epidemiol* **3**, 345-354.

Froshauer, S., Kartenbeck, J. & Helenius, A. (1988). Alphavirus RNA Replicase Is Located on the Cytoplasmic Surface of Endosomes and Lysosomes. *J Cell Biol* **107**, 2075-2086.

Gallagher, S., Winston, S. E., Fuller, S. A. & Hurell, J. G. R. (1998). Immunoblotting and Immunodetection. In *Current Protocols in Immunology*, pp. 8.10.11-18.10.21. New York: John Wiley and Sons, Inc.

Gamarnik, A. V. & Andino, R. (1998). Switch from translation to RNA replication in a positive-stranded RNA virus. *Genes & Dev* **12**, 2293-2304.

Garcia-Briones, M., Rosas, M. F., Gonzalez-Magaldi, M., Martin-Acebes, M. A., Sobrino, F. & Armas-Portela, R. (2006). Differential distribution of non-structural proteins of foot-and-mouth disease virus in BHK-21 cells. *Virol* **349**, 409-421.

Goldstein, L. C., Corey, L., McDougall, J. K., Tolentino, E. & Nowinski, R. C. (1983). Monoclonal Antibodies to Herpes Simplex Viruses: Use in Antigenic Typing and Rapid Diagnosis. *J Infec Dis* **147**, 829-837.

Gorbalenya, A. E., Blinov, V. M., Donchenko, A. P. & Koonin, E. V. (1989). An NTP-binding motif is the most conserved sequence in a highly diverged monophyletic group of proteins involved in positive strand RNA viral replication. *J Mol Evol* **28**, 256-268.

Gorbalenya, A. E. & Koonin, E. V. (1989). Viral proteins containing the purine NTP-binding sequence pattern. *Nucleic Acids Research* **17**, 8413-8440.

Gorbalenya, A. E., Koonin, E. V. & Wolf., Y. I. (1990). A new superfamily of putative NTP-binding domains encoded by genomes of small DNA and RNA viruses. *FEBS lett* **262**, 145-148.

Grubman, M. J. & Baxt, B. (2004). Foot-and-Mouth Disease. *Clin Micro Rev.* **17**, 465-493.

Guinea, R. & Carrasco, L. (1990). Phospholipid biosynthesis and poliovirus genome replication, two coupled phenomena. *EMBO J* **9**, 2011-2016.

Harlow, E. & Lane, D. (1988). *Antibodies: A Laboratory Manual.* Cold Spring: Harbor Laboratory Press.

Harlow, E. & Lane, D. (1999). *Using Antibodies: A laboratory Manual.* New York: Cold Spring Harbor Press.

Harris, K. S., Reddigari, S. R., Nicklin, M. J., Hammerle, T. & Wimmer, E. (1992). *J Virol* **12**, 7481-7489.

Hawkins, D. A., Wilson, R. S., Thomas, B. J. & Evans, R. T. (1985). Rapid, reliable diagnosis of chlamydial ophthalmia by means of monoclonal antibodies. *Brit J Ophth* **65**, 640-644.

Hedman, K., Pastan, I. & Willingham, M. C. (1986). The organelles of the trans domain of the cell. Ultrastructure localizaton of sialogylcoconjugates using *Limax flavus* agglutinin. *J Histochem Cytochem* **34**, 1069.

Hogle, J. M. (2002). Poliovirus cell entry: Common structural themes in viral cell entry pathways. *Ann Rev Microbiol* **56**, 677-702.

Hollinshead, M., Rodger, G., Eijl, H. V., Law, M., Hollinshead, R., Vaux, D. J. & Smith., G. L. (2001). Vaccinia virus utilizes microtubules for movement to the cell surface. *J Cell Biol* **154**, 389-402.

Hornbeck, P. (1991). Enzyme-linked immunosorbent assay. In *Current Protocols in Immunology*, pp. 2.1.2-2.1.22. Edited by J. E. Coligan, A. M. Kruisbeek, D. H. Margulies, E. M. Shevach & W. Strober. New York: John Wiley and Sons, Inc.

Irurzun, A., Perez, L. & Carrasco., L. (1992). Involvement of membrane traffic in the replication of poliovirus genomes: effects of brefeldin A. *Virol* **191**, 166-175.

Janeway, C. A., Travers, P., Walport, M. & Shlomchi, M. J. (2005). *Immunobiology: The immune system in health and disease*. NY and London: Garland Science.

Joachims, M. & Etchison, D. (1992). Poliovirus infection results in structural alteration of a microtubule-associated protein. *J Virol* **66**, 5707-5804.

Johnson, K. & Sarnow, P. (1991). Three poliovirus 2B mutants exhibit noncomplementable defects in viral RNA amplification and display dosage-dependent dominance over wild-type poliovirus. *J Virol* **65**, 4341-4349.

Jouvenet, N. & Wileman, T. (2005). African swine fever virus infection disrupts centrosome assembly and function. *J Gen Virol* **86**, 589-594.

Keck, Z. Y., Machida, K., Lai, M. M., Ball, J. K., Patel, A. H. & Foung, S. K. (2008). Therapeutic control of hepatitis C virus: the role of neutralizing monoclonal antibodies. *Curr Top Microbiol Immunol* **317**, 1-38.

Knox, C., Moffat, K., Ali, S., Ryan, M. & Wileman, T. (2005). Foot-and-mouth disease virus replication sites form next to the nucleus and close to the Golgi apparatus, but exclude marker proteins associated with host membrane compartments. *J Gen Virol* **86**, 687-696.

Koch, M., Niemeyer, G., Patel, I., Light, S. & Nashan, B. (2002). Pharmacokinetics, pharmacodynamics, and immunodynamics of daclizumab in a two-dose regimen in liver transplantation. *Transplantation* **73**, 1540-1646.

Kohler, G. & Milstein, C. (1975). Continuous cultures of fused cell secreting antibodies of predefined specificity. *Nature* **256**, 459-497.

Krogerus, C., Egger, D., Samuilova, O., Hyypia, T. & Bienz, K. (2003). Replication Complex of Human Parechovirus 1. *J Virol* **77**, 8512–8523.

Kuhn, R., Luz, N. & Beck, E. (1990). Functional analysis of the internal translation initiation site of foot-and-mouth disease virus. *J Virol* **64**, 4625-4631.

Langford, G. M. (1995). Actin- and microtubule-dependent organelle motors: interrelationships between the two motility systems. *Curr Opin Cell Biol* **7**, 82-88.

Lee, H., Liu, Y., Mejia, E., Paul, A. V. & Wimmer, E. (2006). The C-Terminal Hydrophobic Domain of Hepatitis C Virus RNA Polymerase NS5B Can Be Replaced with a Heterologous Domain of Poliovirus Protein 3A. *J Virol* **80**, 11343-11354.

Lenk, R. & Penman, S. (1979). The cytoskeletal framework and poliovirus metabolism. *Cell* **16**, 289-301.

Li, J. P. & Baltimore, D. (1990). An intragenic revertant of poliovirus 2C mutant has an uncoating effect. *J Virol* **64**, 1102-1107.

Lipman, N. S., Jackson, L. R., Trudel, L. J. & F.Weis-Garcia (2005). Monoclonal Versus Polyclonal Antibodies: Distinguishing Characteristics, Applications, and Information Resources. *ILAR* **46**, 258-268.

Lipton, H. L. & Friedman, A. (1980). Purification of Theiler's Murine Encephalomyelitis Virus and Analysis of the Structural Virion Polypeptide Profile with Virulence. *J Virol* 33:3. 1165-1172.

Magliano, D., Marshall, J. A., Bowden, D. S., Vardaxis, N., Meanger, J. & Lee, J.-Y. (1998). Rubella Virus Replication Complexes Are Virus-Modified Lysosomes. *Virol* **240**, 57-63.

Martínez-Salas, E., Pacheco, A., Serrano, P. & Fernandez, N. (2008). New insights into internal ribosome entry site elements relevant for viral gene expression. *J Gen Virol* 611–626.

Maynell, L. A., Kirkegaard, K. & Klymkowsky, M. W. (1992). Inhibition of poliovirus RNA synthesis by brefeldin A. *J Virol* **66**, 1985-1994.

McCullough, K. C. & Summerfield, A. (2005). Basic concepts in of immune response and defence development. *ILAR* **46**, 230-240.

Melnick, J. L. (1980). Taxonomy of viruses. *Prog Med Virol* **2**, 214-232.

Mezitis, C. G. M., Steiber, A. & Gonatis, N. K. (1987). Quantitive ultrastructural,autoradiographic evidence for the magnitude and early involvement of the Golgi apparatus complex in the endocytosis of wheat germ agglutinin by cultured neuroblastoma. *J Cell Physiol* **132**, 401-414.

Miller, D. J., Schwartz, M. D. & Ahlquist, P. (2001). Flock House Virus RNA Replicates on Outer Mitochondrial Membranes in Drosophila Cells. *J Virol* **75**, 11664-11676.

Mirzayan, C. & Wimmer, E. (1992). Genetic analysis of an NTP-binding motif in poliovirus polypeptide 2C. *Virol* **189**, 547-555.

Mirzayan, C. & Wimmer, E. (1994). Biochemical Studies on Poliovirus Polypeptide 2C: Evidence for ATPase Activity. *Virol* **199**, 176-187.

Moffat, K., Howell, G., Knox, C., Belsham, G. J., Monaghan, P., Ryan, M. D. & Wileman, T. (2005). Effects of Foot-and Mouth-Disease Virus Nonstructural Proteins on the Structure and Function of the Early Secretory Pathway: 2BC but not 3A Blocks Endoplasmic Reticulum -to-Golgi Transport. *J Virol* **79**, 4382-4395.

Moffat, K., Knox, C., Howell, G., Clark, S. J., Yang, H., Belsham, G. J. & Wilemn, T. (2007). Inhibition of the Secretory Pathway by Foot-and-Mouth DiseaseVirus 2BC Protein Is Reproduced by Coexpression of 2B with 2C, and the Site of Inhibition Is Determined by the Subcellular Location of 2C. *J Virol* **81**, 1129-1139.

Monaghan, P., Cook, H., Jackson, T., Ryan, M. & Wileman, T. (2004). The ultrastructure of the developing replication site in foot-and-mouth disease virus-infected BHK-38 cells. *J Gen Virol* **85**, 933-946.

Murray, L., Luke, G. A., Ryan, M. D., Wileman, T. & Knox, C. (2009). Amino acid substitutions within the 2C coding sequence of Theiler's Murine Encephalomyelitis virus alter virus growth and affect protein distribution. *Virus Research* **144**, 74-82.

Nédellec, P., Vicart, P., Laurent-Winter, C., Martinat, C., Prévost, M. C. & Brahic, M. (1998). Interaction of Theiler's virus with intermediate filaments of infected cells. *J Virol* **72**, 9553-9560

Nieva, J. L., Agirre, A., Nir, S. & Carrasco, L. (2003). Mechanisms of membrane permeabilization by picornavirus 2B viroporin. *FEBS Letters* **552**, 68-73.

Oem, J. K., Yeh, M. T., McKenna, T. S., Hayes, J. R., Rieder, E., Giuffre, A. C., Robida, J. M., Lee, K. N., Cho, I. S., Fang, X., Joo, Y. S. & Park, J. H. (2008). Pathogenic Characteristics of the Korean 2002 Isolate of Foot-and-Mouth Disease Virus Serotype O in Pigs and Cattle. *J Comp Path* **138**, 204-214.

Oleszak, E. L., Chang, J. R., Friedman, H., Katsetos, C. D. & Platsoucas, C. D. (2004). Theiler's Virus Infection: a Model for Multiple Sclerosis. *Clin Micro Rev* **17**, 174-207.

Palmenberg, A. C., Parks, G. D., Hall, D. J., Ingraham, R. H., Seng, T. W. & Pallai, P. V. (1992). Proteolytic processing of the cardioviral P2 region: primary 2A/2B cleavage in clone-derived precursors. *Virol* **190**, 754-762.

Paul, A. V. (2002). Possible unifying mechanism of picornavirus genome replication. In *Molecular Biology of Picornaviruses*, pp. 227-246. Edited by B. L. Semler & E. Wimmer. Washington, DC: ASM Publisher.

Paul, A. V., Molla, A. & Wimmer, E. (1994). Studies of a Putative Amphipathic Helix in the N-Terminus of Poliovirus Protein 2C. *Virol* **199**, 188-199.

Paul, A. V., Reider, E., Kim, D. W., Boom, J. H. v. & Wimmer, E. (2000). Identification of an RNA hairpin in poliovirus RNA that serves as the primary template in the *in vitro* uridylylation of VPg. *J Virol* **74**, 19359-10370.

Pfister, T. & Wimmer, E. (1999). Characterization of the nucleoside triphosphatase activity of poliovirus protein 2C reveals a mechanism by which guanidine inhibits poliovirus replication. *J Biol Chem* **274**, 6992–7001.

Ploubidou, A., Moreau, V., Ashman, K., Reckmann, I., Gonzalez, C. & Way, M. (2000). Vaccinia virus infection disrupts microtubule organization and centrosome function. *EMBO J* **19**, 3932-3944.

Pothier, P., Denoyel, G. A., S.Ghim, deSaint-Maur, G. P. & Freymuth, F. (1986). Use of Monoclonal Antibodies for Rapid Detection of Influenza A Virus in Nasopharyngeal Secretions. *Eur J Clin Microbiol* **5**, 336-339.

Racaniello, V. R. (2001). Picornaviridae: The viruses and their replication. In Fields Virology, 4 edn, pp. 685-722. Philadelphia, USA: Lippincott Williams and Wilkins Publishers.

Restrepo-Hartwig, M. A. & Ahlquist, P. (1996). Brome mosaic virus helicase- and polymerase-like proteins colocalize on the endoplasmic reticulum at sites of viral RNA synthesis. *J Virol* **70**, 8908-8916.

Rhodes, C. H., Steiber, A. & Gonatas, N. K. (1986). A quantitative electron microscopic study of the intracellular localization of wheat germ agglutinin in retinol neurons. *J Comp Neurol* **254**, 287-296.

Rodriguez, P. L. & Carrasco, L. (1993). Poliovirus protein 2C has ATPase and GTPase activity. *J Biol Chem* **268**, 8105-8110.

Rodriguez, P. L. & Carrasco, L. (1995). Poliovirus protein 2C contains two regions involved in RNA binding activity. *J Biol Chem* **270**, 10105-10112.

Rohll, J. B., Moon, D. H., Evans, D. J. & Almond, J. W. (1995). The 3' Untranslated Region of Picornavirus RNA: Features Required for Efficient Genome Replication. *J Virol* **69**, 7835-7844.

Rouiller, I., Brookes, S., Hyatt, A. D., Windsor, M. & Wileman, T. (1998). African Swine Fever Virus Is Wrapped by the Endoplasmic Reticulum. *J Virol* **72**, 2373–2387

Rust, R. C., Landmann, L., Gosert, R., Tang, B. L., Hong, W., Hauri, H. P., Egger, D. & Bienz, K. (2001). Cellular COPII proteins are involved in production of the vesicles that form the poliovirus replication complex. *J Virol* **75**, 9808-9818.

Ryan, M. D., King, A. M. Q. & Thomas, G. P. (1991). Cleavage of foot-and-mouth disease virus polyprotein is mediated by residues located within a 19 amino acid sequence. *J Gen Virol* **72**, 2727-2732.

Ryan, M. D. & Flint, M. (1997). Virus-encoded proteinases of the picornavirus super-group. *J Gen Virol* **78**, 699-723.

Sandoval, I. V. & Carrasco, L. (1997). Poliovirus infection and expression of polivirus protein 2B provoke the disassembly of the Golgi complex, the target for the antipoliovirus drug Ro-090179. *J Virol* **71**, 4679-4693.

Schlegel, A., Giddings, T. H., Ladinsky, M. S. & Kirkegaard, K. (1996). Cellular origin and ultrastructure of membranes induced during poliovirus infection. *J Virol* **70**, 6576-6588.

Skern, T., Hampölz, B., Guarné, A., Fita, I., Bergmann, E., Petersen, J. & James, M. N. G. (2002). *Structure and function of picornavirus proteinases*. Washington, D.C., USA: ASM Press.

Sommergruber, W., Zorn, M., Blaas, D., Fessl, F., Volkmann, P., Maurer-Fogy, I., Pallai, P., Merluzzi, V., Matteo, M., Skern, T. & Keuchler, E. (1989). Polypeptide 2A of human rhinovirus type 2: identification as a protease and characterization by mutational analysis. *Virol* **169**, 68-77.

Stanway, G., Brown, F., Christian, P., Hovi, T., Hyypiä, T., King, AMQ., Knowles, N.J., Lemon, S.M., Minor, P.D., Pallansch, M.A., Palmenberg, A.C., Skern, T. (**2005**). **Family Picornaviridae.** *In* Virus Taxonomy Eighth Report of the International Committee on Taxonomy of Viruses. Edited by: Fauquet, C.M., Mayo, M.A., Maniloff, J., Desselberger, U., Ball. L.A. London: Elsevier Academic Press; 757-778.

Stephan, S., Datta, K., Wang, E., Li, J., Brekken, R. A., Parangi, S., Thorpe, P. E. & Mukhopadhyay, D. (2004). Effect of rapamycin alone and in combination with antiangiogenesis therapy in an orthotopic model of human pancreatic cancer. *Clin Cancer Res* **15**, 6993-7000.

Suhy, D. A., Giddings, T. H. & Kirkegaard, K. (2000). Remodelling the endoplasmic reticulum by poliovirus infection and by individual viral proteins: an autophagy-like origin for virus-induced vesicles. *J Virol* **74**, 8953-8965.

Teterina, N. L., Kean, K. M., Gorbalenya, A. E., Agol, V. I. & Girard, M. (1992). Analysis of the functional significance of amino acid residues in the putative NTP-binding pattern of the poliovirus 2C protein. *J Gen Virol* **73**, 1977-1986.

Teterina, N. L., Gorbalenya, A. E., Egger, D., Bienz, K. & Ehrenfeld, E. (1997). Poliovirus 2C Protein Determinants of Membrane Binding and Rearrangement in Mammalian Cells. *J Virol* **71**, 8962-8972.

Teterina, N. L., Gorbalenya, A. E., Egger, D., Bienz, K., Ehrenfeld, E. & Rinaudo, M. S. (2006). Testing the modularity of the N-terminal amphipathic helix conserved in picornavirus 2C proteins and hepatitis C NS5A protein. *Virol* **344**, 453-467.

Thompson, J.D., Higgins, D.G. & Gibson, J.J. (1994). CLUSTAL W: improving the sensitivity of progressive multiple sequence alignment through sequence weighting, positions-specific gap penalties and weight matrix choice. Nucleic Acid Res **22,** 4673-4680.

Thompson, D., Muriel, P., Russell, D., Osborne, P., Bromley, A., Rowland, M., Creigh-Tyte, S. & Brown, C. (2002). Economic costs of the foot-and-mouth disease outbreak in the United Kingdom in 2001. *Rev Sci Tech* **21**, 675-687.

Torrisi, M. R. & Pinto, S. P. (1984). Compartmentalization of intracellular membrane glycocomponents is revealed by fracture-label. *J Cell Biol* **98**.

Toyoda, H., Nicklin, M. J. H., Murray, M. G., Anderson, C. W., J.J Dunn, Studier, F. W. & EWimmer (1986). A second virus-encoded proteinase involved in proteolytic processing of poliovirus polyprotein. *Cell* **45**, 761-770.

van Kuppeveld, F. J., Melchers, W. J., Kirkegaard, K. & Doedens, J. R. (1997). Structure-function analysis of coxsakie B3 virus protein 2B. *Virol* **227**, 111-118.

Vance, L. M., Moscufo, N., Chow, M. & Heinz, B. A. (1997). Poliovirus 2C Region Functions during Encapsidation of Viral RNA. *J Virol* **71**, 8759-8765.

Voyles, B. A. (2002). *The biology of viruses*.

Wright, C. S. (1984). Structural comparison of the two distinct sugar binding sites in wheat germ agglutinin isolectin II. *J Mol Bol* **178**, 91-104.

Wu, H., Pfarr, D. S., Losonsky, G. A. & Kiener, P. A. (2008). Immunoprophylaxis of RSV infection: advancing from RSV-IGIV to palivizumab and motavizumab. *Curr Top Microbiol Immunol* **317**, 103-123.

Zhai, Z. H., Wang, X. & Qian, X. Y. (1988). Nuclear matrix-intermediate filament system and its alteration in adenovirus-infected HeLa cell. *Cell Biol Int Rep* **12**, 99-108.

Internet: (http://www.physorg.com/news171207257.html), accessed on 19/01/2010